COMPARATIVE STUDY OF TRPM5 IN PANCREATIC ß-CELLS OF WISTAR KYOTO AND GOTO KAKIZAKI RATS

A DISSERTATION SUBMITTED TO THE GRADUATE DIVISION OF THE UNIVERSITY OF HAWAIʻI AT MĀNOA IN PARTIAL FULFILLMENT OF THE REQUIREMENTS FOR THE DEGREE OF

DOCTOR OF PHILOSOPHY

IN

BIOMEDICAL SCIENCES (PHYSIOLOGY)

MAY 2015

By

Mahealani Monteilh-Zoller

Dissertation Committee:

Andrea Fleig, chairperson

Richard Allsop

Reinhold Penner

William Ward

Andy Stenger

ACKNOWLEDGEMENTS

My Heavanly Father and Jesus Christ for creating all things and providing us the agency to do as we see fit.

My husband, Matthew Zoller, for his enduring love, companionship, friendship and support in all I endeavor to do.

My children, Lahaina, Ka'aumoana, Anuenue and Kaiaomalie for loving me and providing me perspective and balance.

My parents, William and Maraea Monteilh for loving me unconditionally and instilling in me the value of responsibility and hard work.

My parents-in-law, Wallace and Marya Zoller and Norma Zoller for their love and support throughout my years as their daughter-in-law.

My mentors and advisors Andrea Fleig and Reinhold Penner for providing me the opportunity to be employed full-time while I pursue my PhD, for your guidance and support throughout the long journey in completing my PhD, for providing a family-friendly work environment, where having to choose between family and work was never an issue.

My committee members, Rich Allsop, Andy Stenger and Steve Ward for your support, your time and your energy in reviewing my thesis.

Department Chair Yusuke Marikawa for reviewing my situation and granting me an extension in completing my PhD.

My grandparents Tuts, Grams, Mom and Pop for their love and support.

My siblings Bill, Anthony, Gino, Vito, Franco, Makalapua and Keao and their respective spouses for their love, support and friendship.

My brothers-in-law, Wallace, Nolan and Derek and their respective spouses for their love, support and friendship.

My Aunts Mildred, Helen, Libbie and Jackie for their love, support, friendship and example.

My Uncles Charles, Kaimi, Bob, Gene, George and Ed for their love, support, friendship and example.

My cousins Leslie, Lana, Leah, Pua, Lilinoe, Healan, Ipo, Lahi and Keala for their love, support and friendship.

My countless other cousins, nieces and nephews from the Ka'alekahi, Monteilh, Zoller and Redulla families for their love, support and friendship.

Dr. Margolskee for providing the TRPM5 antibody.

Malika Faouzi for your support, friendship, humor and for being my editor-in-chief.

Clay Wakano and Aaron Cullen for your support and friendship and for making the lab a nice place to work.

John Starkus for making this lab an interesting place to work, for your sacrifice in time and energy during those many hours trying to perform perforated-patch experiments, for your support and friendship.

Alex Guilloux for your friendship and IT support you provide at the drop of a dime.

Sayuri Suzuki for your support and friendship.

Chad Jansen for your support and friendship and for being my go-to guy when I need reminders on analyzing data in Igor.

Dana Koomoa for providing the islet isolation protocol.

My previous labmates, Henrique Cheng, Andreas Beck, Brett Bessac, Martin Kolisek, Phillippe Demuse, Markus Thiel, Annette Lis, Suzanna Zierler, Lynda Addington, Adriana Sumoza-Toledo, Maurice Needham, Morten Grupe Larson, Rebecca Kim, Jae Won, Lori Tsue, Chris Maggio, Dawn Tani, Tatiana Kilch, Suhel Parvez, Jun Hao Huang, Zheng Zhang, Haijie Yu, Kaohimanu Dang-Akiona, Max Woitok, Lisa Janzon, Stephi Johne, George Myers, Stefan Gross, Ramon Go, Carolyn Oki, Christine Peinelt for your support throughout the years and your lasting friendships.

The staff of IACUC, LAS, Biosafety, for your diligence in caring for our safety and the humane treatment of animals.

The QMC Housekeeping staff for disposing of our biohazard waste regularly.

The QMC Biomed and Facilities staff for keeping our equipment and building in good working order.

The QMC for providing me with partial funding support during my graduate studies.

All the members of my Auwaiolimu Ward family for your love, support and friendship.

The Wistar Kyoto and Goto Kakizaki rats for your sacrifice in making this work possible.

ABSTRACT

TRPM5 is a member of the melastatin subfamily of the Transient-Receptor-Potential superfamily of ion channels. Through functional analysis of the chromosomal region 11p15.5, TRPM5 was identified and linked to a variety of childhood and adult tumors as well as to Beckwith-Wiedemann syndrome (Prawitt et al., 2000). TRPM5 RNA has been detected in a variety of tissues including: taste receptor cells, small intestines, liver, lungs, testis and brain (Hofmann et al., 2003). In addition, the rat insulinoma (INS-1) pancreatic ß-cell line was shown to endogenously express TRPM5 (Prawitt et al., 2003). While earlier studies of TRPM5 conducted in taste receptor cells report TRPM5 as a divalent cation channel that is activated through a G protein-coupled receptor/phospholipase C signaling pathway (Perez et al., 2002; Zhang et al., 2003), other studies (Hofmann et al., 2003; Liu and Liman, 2003) have characterized TRPM5 as a Ca^{2+}-activated non-selective monovalent cation channel.

I here, hypothesize that the pancreatic ß-cells of Goto Kakizaki will exhibit a reduction in TRPM5 which may contribute to the dysfunction of the ß-cell. To this end, we utilized immunostaining to compare the endogenous expression of TRPM5 in the Wistar Kyoto and Goto Kakizaki (spontaneous non-obese type 2 diabetes model) rat pancreatic ß-cell. We also incorporated the whole-cell patch technique to examine the activation characteristics of TRPM5 in both populations of rat ß-cells. Being that TRPM5 is Ca^{2+}-activated, we included fura-2 Ca^{2+} measurements to connect intracellular Ca^{2+}-signaling to TRPM5 activation. In addition, we utilized the perforated patch technique to study glucose-stimulated Ca^{2+}-signaling and TRPM5 activation.

Our results show TRPM5 expression in Wistar Kyoto rat pancreatic ß-cells with expression in the Goto Kakizaki rat being significantly reduced. We also observe significant differences in the glucose-induced Ca^{2+}-signaling in the Goto Kakizaki rat. Our results suggest that chronic hyperglycemia in the Goto Kakizaki rat reduces expression of TRPM5 and leads to pancreatic ß-cell dysfunction thereby contributing to the progression of type 2 diabetes.

TABLE OF CONTENTS

LIST OF DIAGRAMS

LIST OF FIGURES

LIST OF ABBREVIATIONS

ACH: acetylcholine

ADP: adenosine diphosphate

AgCl: silver chloride

AM: acetoxymethyl ester

ATP: adenosine triphosphate

α,ß, δ, γ: alpha, beta, delta, gamma (cell types of the pancreatic islets)

BAPTA: 1,2-Bis (2-Aminophenoxy) Ethane N,N,N'N'-tetraacetic acid

BSA: bovine serum albumin

ºC: degree celsium

Ca^{2+}: calcium ion

$CaCl_2$: calcium chloride

Carbachol: carbamylcholine

CCh: carbachol

Cl^-: chloride ion

CO_2: carbon dioxide

CsCl: cesium chloride

CsOH: cesium hydroxide

DAG: diacylglycerol

DAPI: 4',6-diamino-2-phenylindole

DNA: deoxy-ribonucleic acid

EDTA: ethylenediaminestetraacetate

ER: endoplasmic reticulum

GK: Goto Kakizaki

GLUT-2: glucose transporter 2

G-protein: guanine nucleotide-binding proteins

H^+: hydrogen ion

HEK-293: human embryonic kidney fibroblast cell line

Hz: hertz

I_{max}: maximum current

INS-1: rat insulinoma cell line

IP3: inositol 1,4,5-triphosphate

IP3R: inositol 1,4,5-triphosphate receptor

I/V: current versus voltage relationship

K^+ : potassium ion

K_{ATP}: potassium ATP channel

KCl: potassium chloride

kHz: kilohertz

k_m: Michaelis-Menten constant

L-type: voltage-dependant calcium channel

M3: muscarinic receptor subtype 3

MafA: gene important in pancreatic development and insulin gene transcription

$MgCl_2$: magnesium chloride

mM: millimolar

mOsm: milliosmole

MΩ: megaohm

mRNA: messenger ribonucleic acid

ms: millisecond

mV: millivolt

n: number

Na^+: sodium ion

NaCl: sodium chloride

NADH: reduced nicotinamide adenine dinucleotide

Na^+/K^+ ATPase: sodium-potassium triphosphatase antiporter

nm: nanometer

NaOH: sodium hydroxide

pA: picoamp

PDX-1: pancreatic and duodenal homeobox 1/insulin promoter factor 1

pF: picofarad

PLC: phospholipase C

PIP2: phosphatidylinositol 4,5-bisphosphate

PMCA: plasma membrane calcium ATPase

RCUH: Research Corporation of the University of Hawaii

RNA: ribonucleic acid

ROS: reactive oxygen species

SERCA: sarco/endoplasmic reticulum calcium ATPase

SNARE: SNAp Receptor large protein superfamily which mediate vesicle fusion

TRP: transient receptor potential

TRPC: transient receptor potential canonical

TRPM: transient receptor potential melastatin

TRPM4: transient receptor potential melastatin subfamily 4

TRPM5: transient receptor potential melastatin subfamily 5

TRPML: transient receptor potential mucolipin

TRPN: transient receptor potential no mechanoreceptor potential

TRPP: transient receptor potential polycystic

TRPV: transient receptor potential vanilloid

UV: ultra-violet

μM: micromolar

WK: Wistar Kyoto

CHAPTER 1. INTRODUCTION

1.1. CHANNELS, TRANSPORTERS, POTENTIALS, GRADIENTS

Cells are the basic building blocks of all life. The cell's plasma membrane, with its hydrophobic center and hydrophillic ends, is perfectly suited to separate its intracellular contents from its extracellular environment. A diverse selection of membrane proteins provides the means for regulating the movement of ions and other molecules into and out of the cell.

1.1.1. Transporters and channels are selective, maintaining a cell's resting potential

Ion transporters and ion channels are a class of membrane proteins that serve to maintain the normal ionic and electrical conditions of the cell. A cell typically has a high concentration of potassium ions (K^+) inside the cell relative to its outside and a high concentration of sodium ions (Na^+) outside relative to its inside. This ionic distribution, in turn, contributes to a cell's resting membrane potential of an inside –70 mV. The Na^+/K^+ ATPase is a membrane protein that plays a crucial role in maintaining the ionic distribution and electrical difference that exist across all plasma membranes. The Na^+/K^+ ATPase transporter exchanges 2 K^+ ions into the cell for 3 Na^+ ions out of the cell at the cost of 1 ATP molecule. This type of transport is electrogenic, meaning the exchange of 2 K^+ ions for 3 Na^+ ions results in a charge imbalance where the inside of the cell becomes more negative relative to the outside of the cell.

1.1.2. Gating, ion permeability, conductance and the electrochemical gradient

Ion channels are pores that span the membrane and, when activated, allow the flow of ions down their concentration gradient. Gating mechanisms, ion permeability and conductance are some of the traits used in characterizing ion channels (Minke and Cook, 2002). The gating mechanism describes the opening or closing of an ion channel in response to certain stimulus such as: a voltage change, a chemical or ligand stimulus, a conformational change or a temperature change (Hille, 2001). Once the channel is opened, movement of ions through the pore is determined by the permeability of the channel to the ion (Ashcroft, 2000). Ion permeability is dictated not only by the size and charge of the ion but also by the charge of the amino acid residues located in the narrowest region of the pore (Ashcroft, 2000). Conductance refers to the rate of ion travel through the channel (Hille, 2001). Ions with low conductances bind more tightly to the pore of the channel while ions with high conductances bind less tightly to the pore of the channel (Hille, 2001).

The efficiency of an ion's movement across the plama membrane is dictated by the membrane's permeability to that ion, by the membrane potential and by the concentration difference between the inside and outside of the cell. Every ion has an equilibrium potential. For any ion species, the equilibrium potential is an equal and opposite electrical force required to prohibit the net flow of that particular ion. The resting plasma membrane potential is the sum of every ion's equilibrium potential. In most animal cells, the resting plasma membrane is more permeable to K^+. Being more permeable to K^+ allows not only the intracellular accumulation of K^+ ions but also establishes a resting membrane potential of -70mV, which sits near the equilibrium

potential for K^+ (Hille, 2001). Therefore, the movement of positively charged ions into the cell, with the exception of K^+ ions, is driven by two gradient forces, an electrical gradient and a chemical gradient, collectively termed, the electrochemical gradient. While the tendency for these positive ions to move into the cell exists, this can only be accomplished through the cell's array of aforementioned plasma membrane proteins, namely ion channels, ATP-driven pumps and ion exchangers/transporters.

1.2. TRANSIENT RECEPTOR POTENTIAL MELASTATIN (TRPM)

The Transient Receptor Potential (TRP) superfamily of proteins is made up of more than 20 non-voltage-gated cation channels (Montell et al., 2002). Although these channels are diverse in their gating mechanisms and selectivities, they still share considerable sequence homology and structural similarities (Montell et al., 2002). All members of the TRP superfamily contain six transmembrane segments, a pore loop separating the last two segments and similar lengths of the cytoplasmic and extracellular loops (Harteneck et al., 2000; Montell et al., 2002). They also assemble as tetramers to form complete ion channels. Based on amino acid sequence and structural similarities, channels of the TRP superfamily are divided into six subfamilies which include: TRPC (canonical), TRPV (vanilloid receptor-like), TRPM (melastatin-like), and more recently, TRPP (polycystic), TRPN (nomp) and TRPML (mucolipid) (Fig. 1) (Huang, 2004).

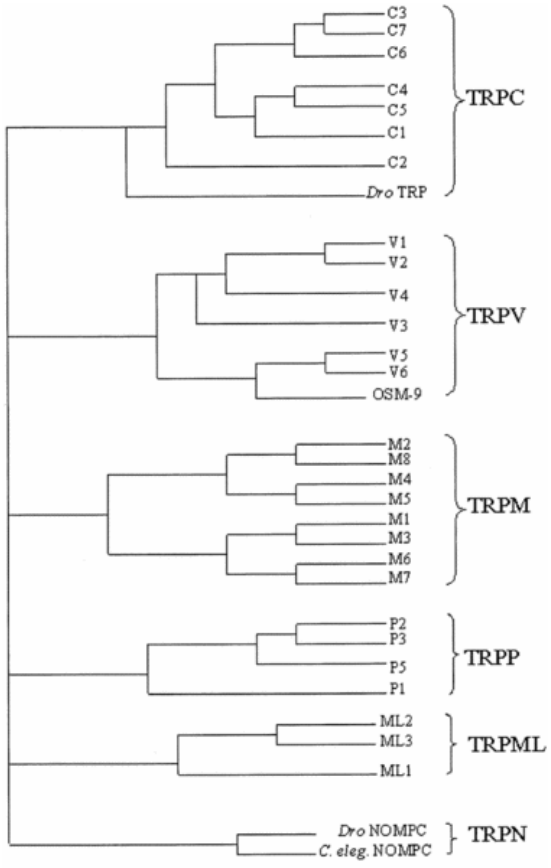

Diag. 1. Phylogenic classification of the transient receptor potential (TRP) superfamily. Huang, 2004.

1.2.1. The TRPM subfamily of channels

The TRPM subfamily of channels is made up of 8 members appropriately named TRPM1 through TRPM8 (Montell et al., 2002). TRPM channels are expressed in a broad array of tissues and have been shown to be involved in many physiological processes ranging from taste transduction in taste buds to magnesium reabsorption in the kidneys and duodenum (Perraud et al., 2001; Walder et al., 2002; Voets et al., 2003; Liu and Liman, 2003).

1.2.2. Transient Receptor Potential Melastatin 5

Through functional analysis of the chromosomal region 11p15.5, TRPM5 was identified and linked to a variety of childhood and adult tumors as well as to Beckwith-Wiedemann syndrome (Prawitt et al., 2000). TRPM5 mRNA has been detected in a variety of tissues with highest expression observed in intestine, pancreas, prostate, kidney and pituitary (Fonfria et al., 2006). In another study, TRPM5 RNA was also shown to be expressed in a variety of tissues that include: taste receptor cells, small intestine, liver, lungs, testis and brain (Hofmann et al., 2003).

Initial characterization of TRPM5 performed by various groups produced contradictory results. A few groups described the channel as a divalent cation channel activated through a G protein-coupled receptor/phospholipase C signaling pathway (Perez et al., 2002; Zhang et al., 2003). Although they agreed that TRPM5 was a divalent cation channel, they disagreed as to the exact activation mechanism of the channel. While one group reported TRPM5 activation through a store-operated mechanism (Perez et al., 2002) the other group reported TRPM5 activation through G-protein coupled receptor that is independent of Ca^{2+}, IP3 and store depletion (Zhang et al., 2003). Later studies have characterized TRPM5 as a Ca^{2+}-activated monovalent nonspecific cation channel (Hofmann et al., 2003; Liu and Liman, 2003). Our work on TRPM5 is to some extent in agreement with the latter studies. In addition to TRPM5 being a Ca^{2+}-activated monovalent nonspecific cation channel, we also reported its activation to be dependent on the rate of change of intracellular Ca^{2+} (Prawitt et al., 2003). An interesting feature of TRPM5 is its transient activation (Prawitt et al., 2003). TRPM5 is fully active within 10 seconds of being exposed to Ca^{2+} (Prawitt et al., 2003). By 40 seconds the current is

nearly abolished (Prawitt et al., 2003). The channel is also modulated by voltage (Prawitt et al., 2003). Because TRPM5 is a nonspecific monovalent cation channel and Na^+ is the ion of abundance extracellularly, the ion carried by the inward current is Na^+ (Prawitt et al., 2003).

TRPM5 was shown to play a role in taste and chemosensing (Perez et al., 2002; Liu and Liman, 2003; Kinnamon, 2009; Ishmaru and Matsunami, 2009; Lin et al., 2008). Taste receptor cells express certain protein receptors that detect sweet, bitter, umami, sour and salt sensations (Huang and Roper, 2010). TRPM5 is co-expressed with taste receptors that sense sweet, umami and bitter tastes and functions to depolarize the basolateral membrane of the receptor cell thereby initiating transmitter release (Ishimaru and Matsunami, 2009). Chemosensory cells of the nasal cavity have been shown to also express TRPM5 (Kaske et al., 2007; Lin et al., 2008; Lin et al., 2008). In this context, TRPM5 is believed to be a signaling component in the detection of airborne irritants (Lin et al., 2008).

A hint that TRPM5 may play a role in pancreatic ß-cell function came about when a variety of human, murine and rat cell lines from various organs were analyzed for endogenous TRPM5 transcripts (Prawitt et al., 2003). The rat insulinoma (INS-1) pancreatic ß-cell line was among a few shown to endogenously express TRPM5 (Prawitt et al., 2003). In this study, INS-1 cells demonstrated the presence of a current with TRPM5-like traits, having an outwardly rectifying Ca^{2+}-activated current (Prawitt et al., 2003). More recently, the role of TRPM5 in primary pancreatic ß-cells has been studied more extensively (Colsoul et al., 2010; Brixel, et al., 2010). Both studies conclude TRPM5 plays a key role in glucose-stimulated insulin secretion. More specifically,

Colsoul and colleagues report TRPM5 as an essential component in high frequency Ca^{2+} oscillations. These high frequency Ca^{2+} oscillations are believed to be more efficient in triggering exocytosis of secretory vesicles than slow oscillations (Berggren et al., 2004).

1.3. THE ENDOCRINE PANCREAS AND INSULIN SECRETION

The pancreas is an organ that performs both exocrine and endocrine functions (Berne and Levy, 1998). Pancreatic exocrine juice is comprised of digestive enzymes and neutralizing bicarbonate. The exocrine pancreas serves two purposes: (1) digest carbohydrates, proteins and fats and (2) neutralize duodenal contents (Berne and Levy, 1998). The endocrine pancreas is made up of clusters of cells, collectively termed Islets of Langerhans. While they are responsible for the tremendous task of regulating blood glucose levels, Islets of Langerhans make up less than 2% of the entire pancreas (Berne and Levy, 1998). The Islets of Langerhans are comprised of 4 different cells types: alpha cells (α-cells), beta cells (ß-cells), delta cells (δ-cells) and gamma cells (γ-cells). These cells are distinguishable according to the hormones they secrete. Alpha (α) cells secrete glucagon, δ-cells secrete somatostatin, γ-cells secrete a pancreatic polypeptide and ß-cells secrete insulin. Within the Islets of Langerhans, ß-cells have been shown to make up ~80% of the cell population (Baetens et al., 1979; Bonner-Weir, 1989; Weir and Bonner-Weir, 1990).

1.3.1. Blood glucose and hormones of the endocrine pancreas

Whether directly or indirectly, all the hormones of the endocrine pancreas affect blood glucose levels. Pancreatic polypeptide release from γ-cells is triggered by protein-rich meals, fasting, exercise and acute hypoglycemia and is inhibited by somatostatin and intravenous glucose (Batterham et al., 2003). While the exact physiological role of pancreatic polypeptide is unclear, some studies have suggested pancreatic polypeptide acts as an appetite suppressor (Batterham et al., 2003; Jesudason et al., 2007). Somatostatin is secreted by a broad range of tissues including pancreas, intestine and brain (Brazeau et al., 1973; Kumar et al., 1999). Although somatostatin may originate in different tissues, its effects on these tissue are largely inhibitory (Brazeau et al., 1973; Kumar et al., 1999). For example, somatostatin from pancreatic δ-cells acts in a paracrine fashion to inhibit the synthesis and secretion of insulin and glucagon from ß- and α-cells, respectively (Dubois, 1975; Mandarino et al., 1981).

Blood glucose, insulin and glucagon are all interrelated and very tightly regulated by one another through feed back loops (Berne and Levy, 1998). Therefore, both insulin and glucagon are responsible for directly regulating blood glucose levels and in turn, the level of blood glucose regulates whether insulin or glucagon are secreted (Berne and Levy, 1998). Insulin and glucagon target tissues include: liver, muscle and adipose (Berne and Levy, 1998). In healthy individuals, blood glucose levels are maintained between 70 and 100 mg/dl (3.9 and 5.6 mM) during the fasting state and reaches levels no higher than 140 mg/dl (7.8 mM) after consuming a meal (Kruger et al., 2006). Glucagon is secreted in response to blood glucose deficiency or hypoglycemia, where

blood glucose falls below 55 mg/dl (3 mM), and thereby acts to maintain normoglycemia by increasing circulating levels of glucose (Berne and Levy, 1998). Although insulin secretion is controlled by a number of factors, an elevation in blood glucose is the main effector (Berne and Levy, 1998). Plasma glucose and insulin levels are so closely associated that their relationship is sigmoidal in nature (Berne and Levy, 1998). At plasma glucose levels of 50 mg/dl, almost no insulin is secreted (Berne and Levy, 1998). Half-maximal and maximal insulin secretion occur at 150 mg/dl and 300 mg/dl glycemic levels, respectively (Berne and Levy, 1998). Following a meal, insulin lowers blood glucose by 4 mechanisms: (1) insulin stimulates glucose uptake in muscle cells and adipocytes; (2) insulin stimulates glucose storage in the liver in the form of glycogen; (3) insulin inhibits glucagon secretion, thereby suppressing glycogenolysis and (4) insulin directly inhibits glucose production in the liver (Kruger et al., 2006).

1.3.2. Insulin secretion is pulsatile

A distinguishing feature of the ß-cell is that insulin secretion occurs in a pulsatile manner (Chou and Ipp, 1990; Goodner et al., 1977). The pulsatile nature of insulin secretion is important in preventing down regulation of insulin receptors in target tissues (Perksen et al., 2002; Komjati et al., 1986). The ability to generate oscillatory signals is inherent in ß-cells (Grapengiesser et al., 1989; Nilsson et al., 1996; Ainscow et al., 2002). The source of these oscillatory signals is a complex yet coordinated interplay between ion channels (Hiriart and Aguilar-Bryan,2008), intracellular Ca^{2+} levels (Bergsten, 1995) and metabolic substrates (Tornheim, 1988; Tornheim, 1997). The enzymatic activity of

phosphofructokinase is seen as a key regulatory step in glycolysis thereby playing a major role in the oscillatory production of pyruvate (Tornheim, 1988). Fluctuations in pyruvate lead to fluctuations in ATP production (Tornheim, 1988). As mentioned previously, ATP accumulation will depolarize the plasma membrane. Conversely, when intracellular ATP levels drop, the plasma membrane will not depolarize. Hence ultimately leading to fluctuations in insulin secretion (Tornheim, 1988).

1.4. CALCIUM AND THE PANCREATIC ß-CELL

Calcium is the primary signaling element of all cells. Intracellular Ca^{2+} signaling is involved in a wide range of cellular processes that include muscle contraction, neurotransmitter release, an immune response and secretion. Although Ca^{2+} is the driving force behind many crucial events, prolonged elevation has cytotoxic effects. In order to fulfill its role as a second messenger, yet not be toxic to the cell, Ca^{2+} must remain an intracellular limiting factor and must also be readily available. A cell has evolved mechanisms that address these issues by maintaining an intracellular free Ca^{2+} concentration of ~100 nM which results in a 10,000-fold extracellular-to-intracellular Ca^{2+} gradient. In addition, within the cell itself, Ca^{2+} is sequestered in the endoplasmic reticulum at a concentration that produces a similar 10,000-fold gradient. Calcium entry into cells occurs through the vast array of ion channels that include voltage-operated, store-operated and receptor-operated Ca^{2+} channels. For Ca^{2+} moving from the endoplasmic reticulum to the cytosol, the common pathway is through the $InsP_3$ (IP3) or ryanodine receptors. For the removal of Ca^{2+} from the cytosol, the cell has the plasma

membrane Ca^{2+} ATPase (PMCA) or the sarco(endo)plasmic reticulum Ca^{2+} ATPase (SERCA) pumps to either extrude Ca^{2+} from the cell or sequester Ca^{2+} in the endoplasmic reticulum, respectively.

1.4.1. Membrane potential, intracellular Ca^{2+} signals and ion channels in ß-cells

The general consensus model of glucose-stimulated insulin secretion occurs following a meal as glucose is transported into pancreatic ß-cells through the Glut-2 transporter (Berne and Levy, 1998). Glucose is then subjected to glycolysis to form pyruvate, ATP and NADH (Berne and Levy, 1998). Pyruvate then progresses through to the citric acid cycle and a build up of intracellular ATP occurs. This increase of ATP leads to a decrease in the intracellular ADP/ATP ratio and the subsequent closure of the K_{ATP} channel. In the absence of ATP, the K_{ATP} channel is open and conducts K^+ ions out of the cell to maintain the –70mV membrane potential. With the closure of the K_{ATP} channel, K^+ ions no longer outwardly permeate the membrane causing the membrane to depolarize. This leads to the activation of voltage-dependent L-type Ca^{2+} channels, calcium influx and insulin secretion via SNARE proteins.

The pancreatic ß-cell is characterized as being electrically active, thereby having the ability to generate action potentials. More specifically, the electrical activity of the beta cell is characterized as oscillating between hyperpolarized potentials and depolarized plateaus upon which bursts of action potentials are superimposed (Valdeolmillos et al., 1996). Beta cell electrical activity occurs in response to glucose and other secretogogues and is dictated by a complex yet coordinated interplay between ion channels, transporters and pumps (Ashcroft and Rorsman, 1989). At the center of ß-cell electrical activity is the

K_{ATP} channel. Adenosine-5'-triphosphate, the intracellular energy currency, is produced during glucose metabolism. Blood glucose levels dictate intracellular ATP levels, which in turn dictate the activity of the K_{ATP} channel. In the presence of low glucose (less than 3 mM), the pancreatic ß-cell resting membrane potential is mainly due to the activity of K_{ATP} channels and the electrogenic Na^+/K^+ ATPase transporter and therefore sits near –70 mV (Ashcroft and Rorsman, 1989). At glucose concentrations greater than 7 mM, an increase in intracellular ATP occurs. This results in the closing of the K_{ATP} channel and membrane depolarization to approximately –50 mV (Ashcroft and Rorsman, 1989).

The Ca^{2+} signal is the result of an organized sequence of Ca^{2+} release from intracellular stores and Ca^{2+} influx across the plasma membrane. Calcium acts as an intracellular second messenger when it is mobilized in the cytosol either through release from the endoplasmic reticulum or through influx via Ca^{2+} channels. The most common Ca^{2+} signaling pathway that increases cytosolic Ca^{2+} involves the G-protein-coupled phospholipase C pathway followed by store-operated calcium influx. In this pathway, a G(q)-protein is stimulated and activates the membrane-bound phospholipase C enzyme. The enzyme hydrolyzes phosphatidylinositol 4,5-bisphosphate (PIP2) to form Inositol 1,4,5-triphosphate (IP3) and Diacylglycerol (DAG). IP3 binds to and opens the IP3 receptor of the endoplasmic reticulum (ER). Calcium is then released from the ER into the cytosol. Following Ca^{2+} release, store-operated Ca^{2+} influx occurs through Ca^{2+} channels.

The L-type Ca^{2+} channel couples membrane electrical excitability with calcium influx in a variety of electrically excitable cells including pancreatic ß-cells. The L-type Ca^{2+} channel is the main avenue by which calcium permeates the ß-cell plasma

membrane (Ashcroft et al., 1994). With the basal calcium level of a resting cell sitting at approximately 100 nM, the cell utilizes the electrochemical gradient across the plasma membrane in conjunction with the L-type Ca^{2+} channel to bring about Ca^{2+} influx.

1.4.2. Calcium and Exocytosis

Calcium is an important element in many cellular events with its effects dependant upon the cell's function. Pancreatic ß-cells are considered secretory cells and calcium's role in these cells is to mediate binding of intracellular proteins necessary for the actual secretion of insulin. The general term used in describing insulin secretion is exocytosis and it's the process whereby the cell can extrude intracellular molecules to the extracellular environment. Exocytosis involves the docking and fusion of vesicles with the plasma membrane through the respective interaction of synaptotagmin with SNARE complexes (Hou et al., 2009). Complexin, a protein included with the SNARE complex, inhibits the interaction between synaptotagmin and the SNARE complex. In the presence of calcium, synaptotagmin displaces complexin from the SNARE complex and vesicle fusion ensues (Hou et al., 2009).

The major sources of Ca^{2+} available for exocytosis are located internally, in the endoplasmic reticulum and externally, in the extracellular matrix. The source of Ca^{2+} determines the action of Ca^{2+} in insulin secretion. It has been shown that L-type Ca^{2+} channels bind to SNARE proteins (Wiser, et al., 1999). This binding enables the Ca^{2+} that enters through L-type channels to be readily available to sites of exocytosis (Wiser, et al.,

1999). Ca^{2+} that originates from the endoplasmic reticulum is believed to play a role in amplifying insulin secretion and replenishing the pools of insulin granules (Gromada et al., 1999).

1.5. NEURONAL CONTROL OF ß-CELLS AND THE CA^{2+}_{i} SIGNAL

1.5.1. Pancreatic islets are innervated by parasympathetic and sympathetic nerves

The endocrine pancreas receives rich input from sympathetic and parasympathetic nerves (Ahren, 2000; Brunicardi et al., 1987). In general, the sympathetic nervous system acts to increase blood glucose under conditions of stress not only by inhibiting insulin secretion but also by stimulating glucagon secretion (Ahren, 2000). On the other hand, the parasympathetic nervous system acts to lower blood glucose by stimulating insulin secretion (Gilon and Henquin, 2001). Therefore, aside from glucose, other physiological agents such as neurotransmitters also influence insulin secretion.

1.5.2. Pancreatic ß-cells express the M3 muscarinic receptor

In addition, rat pancreatic islets have been shown to express m1 and m3 muscarinic receptors (Iismaa et al., 2000). While both receptors are expressed in equal amounts in pancreatic ß-cells (Iismaa et al., 2000), the m3 receptor subtype is believed to be involved in the parasympathetic regulation of insulin secretion (Boschero et al., 1995; Verspohl et al., 1990). Carbamylcholine (carbachol) is an agent that mimics the parasympathetic neurotransmitter acetylcholine and binds to both m1 and m3 muscarinic receptors (Iismaa et al., 2000). Interaction of carbachol with the m3 muscarinic receptor

leads to G_q-coupled activation of phospholipase C. Phospholipase C hydrolyzes phosphatidylinositol 4,5-bisphosphate (PIP2) to form inositol 1,4,5-triphosphate (IP3) and diacylglycerol (DAG). IP3 enters the cytoplasm and activates IP3 receptors of the smooth endoplasmic reticulum leading to Ca^{2+} release from these intracellular Ca^{2+} stores. The Ca^{2+} from these intracellular stores are involved in different pathways within the ß-cell which can effect capacitative Ca^{2+} entry or activation of Ca^{2+}-dependent ion channels which ultimately lead to insulin secretion.

1.6. TYPE 2 DIABETES

1.6.1. ß-cell dysfunction and insulin resistance

Type 2 diabetes affects an estimated 150 million individuals worldwide and is predicted to double within 20 years (Zimmet et al., 2001). In type 2 diabetes, individuals have lost the ability to effectively regulate blood glucose (Kruger et al., 2006). Because insulin is responsible for reducing blood glucose, it is believed that insulin resistance and ß-cell dysfunction both contribute to the development of the disease (Kahn, 2003). Insulin resistance occurs when normal amounts of insulin become inadequate to elicit a normal glucose uptake response in target tissues like muscle and liver (Abdul-Ghani et al., 2006). Insulin resistance is influenced by a number of different factors such as: genetics, age, diet, physical fitness, medication, obesity and fat distribution (Kahn, 2003). Defects in the normal pattern of insulin secretion, impairment of feedback control between glucose and insulin secretion and an abnormal pattern of expression for islet genes are all indications of ß-cell dysfunction (Tokuyama et al., 1995). Because insulin

resistance and ß-cell dysfunction do not occur independent of one another, it is difficult to ascertain the relative contributions and timing of both abnormalities in the development of type-2 diabetes (Bell et al., 2001 and Kahn, 2003). Although this is the case, Tokuyama et al (1995) have shown that multiple defects in ß-cell gene expression are observed in prediabetic animals, suggesting that ß-cell dysfunction occurs well before the development of hyperglycemia.

1.6.2. Chronic hyperglycemia affects gene expression

Individuals with type 2 diabetes exhibit chronic hyperglycemia. Hyperglycemia is characterized by a blood glucose level higher than 180 mg/dl (10 mM). Chronic hyperglycemia is a classic sign of type 2 diabetes. Chronic exposure of ß-cells to high levels of glucose leads to ß-cell dysfunction by altering gene expression. There are a plethora of cellular events that occur to render the pancreatic ß-cell defective. Although the origin of the ß-cell's lack of glucose responsiveness is not exactly known, some observations report insulin expression, during a high glucose challenge, is insufficient in compensating for such an increase in glucose levels (Hribal et al., 2003). Under physiological conditions mammalian homologue of avian MafA (MafA) and pancreatic duodenal homeobox factor 1 (PDX-1) are two critically important transcription factors of insulin promoter activity (Olson et al., 1993; Portout et al., 1996).

There are a plethora of cellular events in which the defective pancreatic ß-cell must overcome to achieve normoglycemia. Islets intrinsically express low levels of antioxidant enzymes such as superoxide dismutase, catalase and glutathione peroxidase (Lenzen et al., 1996). This intrinsic trait thereby increases the risk of oxidative damage

from the formation of reactive oxygen species that result from the phosphorylation of glucose. This low anti-oxidant gene expression may provide some light to the sensitivity pancreatic ß-cells have towards reactive oxygen species Insulin promoter PDX-1 gene transcription normal but PDX-1 mRNA PDX-1 protein, insulin RNA and Insulin content diminished, indicates postranscriptional loss of PDX-1 mRNA. Under physiological conditions MafA and PDX-1 are two critically important regulators of insulin promoter. Loss of MafA binding was associated with normal levels of MafA mRNA. The abnormality was the absence of the MafA protein, which indicates a posttranslational loss of MafA as the mechanism of action.

No changes were observed in expression of molecules involved in glucose sensing such as GLUT2 and glucokinase. This indicates that defects in insulin secretion caused by elevation in ambient glucose levels are not the result of altered expression of key proteins involved in glucose sensing, but of alterations in intracellular mechanisms of glucose stimulated insulin release. Steady state insulin mRNA levels were not increased in human islets exposed to high glucose levels compared with controls. Human islets exposed to high glucose failed to compensate by increasing insulin transcription for sustained secretory demand secondary to elevations in ambient glucose concentrations (Hribal et al., 2003).

The pathophysiological implication of the islet's intrinsically low level of antioxidant enzyme expression and activity is that the beta cell is at greater risk of oxidative damage than other tissues with higher levels of antioxidant protection. A higher concentration of glucose was shown to increase the level of intracellular peroxide levels within the islet (Tanaka et al., 2002). These observations agree with those of Ihara et al

(Ihara et al., 1999) who reported elevated levels of oxidative stress markers in ß-cell of Goto Kakizaki rats. ROS that might be formed include superoxide, hydrogen peroxide, nitric oxide, and hydroxyl radicals. Among these, the hydroxyl radical is the most toxic because it easily passes through membrane barriers to the cell's nucleus and strongly reacts mutagenically with DNA.

1.7. AIMS OF THIS STUDY

Pancreatic ß-cells are highly sensitive to changes in blood glucose. They secrete insulin in response to an increase in blood glucose to maintain glucose homeostasis. The ß-cell is also electrically excitable and the process of insulin secretion involves a complex interplay of ion channels. Insulin secretion is initiated by a depolarizing change in the ß-cell and because ion channels are at the center of all cellular electrical activity, ion channels are one of the key elements in insulin secretion.

1.7.1. TRPM5 in Wistar Kyoto rat pancreatic ß-cells

Although the K_{ATP} channel conductance dominates ß-cell resting potential, it is the interaction between various ion channels that determines ß-cell electrical activity (Ashcroft and Rorsman, 1989). Because a direct correlation exists between the extent of ß-cell electrical activity and the amount of insulin secretion (Henquin and Meissner, 1984), we believe TRPM5 plays a role in rat pancreatic ß-cell insulin secretion by converting an intracellular Ca^{2+} signal into an electrical signal by contributing to a transient depolarizing membrane potential. This study will aim to examine the role of TRPM5 in the Wistar Kyoto rat pancreatic ß-cell.

1.7.2. TRPM5 in Goto Kakizaki rat pancreatic ß-cells

I hypothesize that an impaired TRPM5 leads to a decline in membrane depolarization thereby playing a role in ß-cell dysfunction. The Goto Kakizaki rat is a spontaneous animal model of non-insulin dependent diabetes mellitus (type 2 diabetes) without obesity (Goto et al., 1988). This model was produced by repeated selective breeding between glucose intolerant rats from a nondiabetic Wistar Kyoto colony (Goto et al., 1988) and develops type 2 diabetes at approximately 14-16 weeks of age. This model will enable us to study the effects of diabetes on TRPM5. We will also be able to measure any differences in TRPM5 expression and activity between pancreatic ß-cells of Wistar Kyoto and Goto Kakizaki rats.

CHAPTER 2. MATERIALS AND METHODS

2.1. CELLS

Islets of Langerhans contain the endocrine cells of the pancreas and make up about 1-2% of the entire pancreas. Within the islets, the insulin secreting ß-cells, make up about 80% of the cell mass. Pancreatic ß-cells were isolated weekly. We isolated cells from male Wistar Kyoto rats or Goto Kakizaki rats whose age was at least 16 weeks. We selected 16 week or older rats to ensure that the Goto Kakizaki rats were indeed diabetic.

The endocrine pancreas makes up only 1-2% of the entire pancrease and the remaining portion of the pancreas is comprised of exocrine tissue. Pancreatic exocrine tissue digestion from Wistar Kyoto and Goto Kakizaki was initiated with intraductal perfusion of 0.25 mg/ml collagenase type xi (Sigma catalog number C7657) in 0.5% Albumin, Bovine Serum, Fraction V (Calbiochem catalog number 12659) in Hanks Balanced Salt Solution (Media Tech catalog number MT21023CV). Islets were then individually hand picked. Following digestion with 0.25% Trypsin-EDTA (Sigma catalog number T4049), islet ß-cells were subseqeuntly plated on polylysine (Sigma catalog number P8920) coated coverslips and allowed to recover in RPMI-1640 (Media Tech catalog number MT 10043CV) containing 10% Fetal Bovine Serum (Invitrogen catalog number 16140071) in 37ºC in a 5% CO_2 humidified incubator overnight. In experiments examining the effect of high glucose, the culture medium contained 10 mM glucose. Experiments were performed on these cells from 16 hours to 3 days following isolation.

2.2. SOLUTIONS

Extracellular solutions for whole-cell patch-clamp and Ca^{2+} measurement experiments consisted of a standard Ringer's solution comprised of the following: 140 mM NaCl (Sigma catalog number S9888), 2.8 mM KCl (Sigma catalog number P9333), 2 mM $MgCl_2$ (Sigma catalog number M1028) and 10 mM Hepes-NaOH (Sigma catalog number H3375 and Fisher catalog number SS255-1) solution that contained 4 mM glucose (Sigma catalog number G8270), 10 mM CsCl (Fisher catalog number BP210) and 1 mM $CaCl_2$ (Sigma catalog number 4901); pH 7.2, 300-330 mOsm. The osmolarity of our solutions was measured using a vapor pressure osmometer (Wescor). Filtered extracellular Ringer's solution was also used for experiments involving the application of a compound (20 μM ionomycin (Sigma catalog number I0634), 100 μM carbamoylcholine chloride (Sigma Aldrich catalog number C4382), 4 mM glucose and 16.7 mM glucose (Sigma catalog number G8270)) to the cell's extracellular surface. In these cases, filtered extracellular Ringer's solution was used to solubulize the compound of interest.

Intracellular solutions for whole-cell patch-clamp experiments consisted of a cesium-based Ringer's solution comprised of the following: 140 mM L-(+)-glutamic acid (Fisher Scientific catalog number A125), titrated with cesium hydroxide (Sigma catalog number 21351-79), 8 mM NaCl (Sigma catalog number S9888), 1 mM $MgCl_2$ (Sigma catalog number M1028) and 10 mM Hepes-CsOH solution (Sigma catalog number H3375 and Sigma catalog number 21351-79); pH 7.2, 300-330 mOsm. Experiments measuring intracellular Ca^{2+} levels utilized 200 μM Fura-2 pentapotassium (Life Technologies catalog number F1200) solubolized in the cesium-based Ringer's solution.

In examining the effects of various concentrations of free Ca^{2+} on the activation of endogenous TRPM5 in rat pancreatic ß-cells, we used 10 mM 5,5'-Dibromo BAPTA (Invitrogen catalog number, D1211) to buffer the intracellular solution to a certain free Ca^{2+} concentration. The on-line WEBMAXC STANDARD program was utilized in calculating free Ca^{2+} values.

2.3. IMMUNOSTAINING

Immunostaining of pancreatic ß-cells was employed to examine the endogenous expression patterns of TRPM5 in the Wistar Kyoto and the Goto Kakizaki rat. All reagents for the fixation, blocking, permeablelization and staining were prepared using Hank's Balanced Salt Solution (Media Tech catalog number MT21023CV). Cells were allowed to recover for 16 hours following isolation before being subjected to a 2% paraformaldehyde (Sigma catalog number 158127) cellular fixation. To block for non-specific binding of the primary antibody we utilized 2% bovine serum albumin (Sigma catalog number A2153). To permeablelize the cell membrane, we utilized 0.2% triton X-100 (Sigma catalog number X100). We utilized a ß-cell surface-specific monoclonal antibody K14D10 (Enzo Life Sciences, catalog number ALX-803-052-C100) and an antibody against TRPM5. In order to determine the specificity of the two primary antibodies for viable rat pancreatic ß-cells and TRPM5, the pancreatic ß-cells were secondarily exposed to the fluorophores Alexa Fluor 568 (anti-mouse) (Invitrogen, catalog number, A11031) for K14D10 binding and Alexa Fluor 488 (anti-rabbit) (Invitrogen, catalog number, A11034) for TRPM5 expression. In order to visualize intact DNA of the cells, DAPI staining using the ProLong Gold Antifade Reagent (Invitrogen,

catalog number, P-36931) was utilized in mounting the cells to microscope slides. Images were obtained using a Zeiss LSM 5 Pascal Confocal Microscope (RCUH-Core Facility).

2.4. PATCH-CLAMP ELECTROPHYSIOLOGY

2.4.1. Whole-cell configuration of the patch-clamp technique

In the patch clamp technique, the cell membrane represents a capacitor with variable resistors (ion channels). The patch clamp technique allows for the measurement of small currents generated when ions move through ion channels. In order to be able to measure the currents across the cell membrane, electrodes must be placed within the cell (glass recording electrode) and outside the cell (bath reference electrode). The electrode located outside the cell sits in the bath and is a AgCl-coated silver wire. The electrode that is placed within the cell is made of glass that has been pulled and fire-polished at the tip. Fire polishing is essential for the formation of a very tight giga-seal between the cell membrane and the glass electrode. The glass electrode is pulled using the Sutter glass puller with a resulting size resistance of abut 2.5 MΩ. The glass electrode is also filled with intracellular Ringer's solution and has a AgCl-coated silver-wire that can manipulate the internal voltage of the cell and measure the currents that flow across the membrane. The current signal measured by the glass electrode is filtered at 2.3 kHz and amplified. The amplified signal is then converted to a digital signal by a computer-based amplifier signal (EPC-10, HEKA). With computer software (Pulse + PulseFit), we were able to set the electrical parameters of the experiment and measure the resulting currents across the plasma membrane, presumably through ion channels.

For the patch-clamp electrophysiological experiments performed in this project, cells were held at either -40 mV or 0 mV and given a voltage ramp protocol from -100 mV to +100 mV for 50 ms, every other second. The currents that develop during the ramp at -80 mV and +80 mV were recorded and reported in the Results section. Currents measured at -80 mV are currents expected at a cell's resting potential. We utilized Igor Pro (version 6.34) in analyzing our currents obtained at -80 mV and +80 mV. P-values were obtained using Microsoft Excel version 14.1.0.

Cells were plated on poly-lysine coated coverslips. Coverslips were secured into petri-dish patch chambers using a small amount of silica. The patch chamber was filled with approximately 2.5 ml of extracellular Ringer's solutions and loaded onto the patch-clamp apparatus. Cells were visible through a microscope (Axiovert 35, Zeiss) as well as through a high resolution ccd camera (Javelin) connected to a monitor (Sony). The stage of the microscope was motorized and connected to an Eppendorf micromanipulator (model 5171). This apparatus enabled the ability to visualize cells on a monitor and move the patch chamber to select cells for experiments. The bath reference electrode was secured in the patch chamber. The glass electrode was filled with intracellular Ringer's solution and mounted onto the AgCl-silver wire which is also mounted onto a motorized arm controlled by the Eppendorf micromanipulator. The glass electrode apparatus is connected to a tubing to apply suction to form the Giga-seal.

Once a cell is selected, the glass electrode is placed into the bath. Upon entry into the bath, the glass electrode applies voltage-clamp test pulses at +10 mV and -10 mV for 20 milliseconds each. These test pulses allows the resistance or size of the glass electrode tip to be determined and its usually between 2.5-3.0 MΩ. The difference between the

charges of the solutions that exists in the glass electrode and the bath solution was accounted for with a liquid junction of 10 mV. The glass electrode is manipulated and lightly placed upon the cell. Slight suction is applied and a large resistance between the glass electrode tip and the cell membrane develops to at least 1 GΩ.

The formation of the giga-seal renders the cell ready to be perfused with the intracellular Ringer's solution with the glass electrode. To gain access to the inside of the cell, the patch of membrane that is isolated within the glass electrode tip opening must be broken. By providing repeated quick pulses of suction the patch of membrane is broken and access to the inside of the cell is gained without losing the giga-seal. The glass electrode clamps the voltage of the cell and records the current that flows across the membrane.

2.4.2. Application of compounds during whole-cell patch-clamp experiments

The patch-clamp apparatus is very functional in that it allows the manipulation of the extracellular environment during recordings. A second glass application pipet can be prepared which contains the compound of interest. This glass application pipet is connected to a pressure pump (Lorenz) which applies positive pressure to release the compound into the surrounding environment of the cell. In the case of our current studies, the glass application pipet contained either 20 μM ionomycin (Sigma), 16.7 mM glucose (Sigma) or 100 μM carbachol (Sigma). These compounds were applied typically when current baseline was established and stable between 60-100 seconds.

2.4.3. Fura-2 measurements during whole-cell patch-clamp experiments

Because TRPM5 is a Ca^{2+}-activated channel, utilizing Fura-2 to establish the connection between intracellular Ca^{2+} signaling and TRPM5 activation was possible. Fura-2 is a UV-excitable fluorescent indicator used to measure free intracellular concentrations of Ca^{2+}. Fluorescent signals were sampled at 5 Hz with a photomultiplier-based system using a monochromatic light source (TILL Photonics) tuned to excite at 340 and 380 nm. The analog emissions were detected at 450-550 nm with a photomultiplier and were converted with a digital-analog interface (ITC-16, Instrutech). The fluorescent ratios (340/380) were processed and converted to free Ca^{2+} concentrations by X-Chart software (HEKA). In these sets of experiments, cells were perfused with standard intracellular pipette solution containing 200 μM Fura-2.

We also utilized the perforated-patch technique to measure intracellular Ca^{2+} without disrupting the intracellular environment. Cells were loaded with 5 μM Fura-2-AM (acetoxymethylester, Invitrogen) for 30 minutes in media at 37 °C. Cells were then subjected to freshly prepared 80 μM amphotericin B (Sigma, A2411) through the glass pipet electrode. Cells were kept in the cell attached mode at a 0 mV holding potential until the series resistance decreased to less than 20 MΩ (10-15 minutes). Once the desired series resistance was obtained, we initiated the standard ramp protocol as mentioned above. Fluorescent measurements were recorded during the experiment. Cells were then exposed to stimulatory glucose to examine the effects of glucose on intracellular Ca^{2+} signaling and TRPM5 activation.

In our analysis of calculating free calcium concentration or calcium ratios, we utilized we utilized Igor Pro (version 6.34) in analyzing. We also utilized Microsoft Excel version 14.1.0 to obtain our p-values.

2.5. FLUORESCENT MEASUREMENTS IN INTACT CELLS

Cells were loaded with 5 μM Fura-2-AM (acetoxymethylester, Invitrogen) for 30 minutes in media at 37 °C and were exposed to 16.7 mM glucose. Measurement of intracellular free Ca^{2+} was performed as mentioned above.

CHAPTER 3. RESULTS

The INS-1 cell line is derived from the rat pancreatic ß-cell. Because it expressed the TRPM5 transcript and also possessed a TRPM5-like current, there is a strong possibility that TRPM5 is endogenously expressed in Wistar Kyoto rat pancreatic ß-cells. The Goto Kakizaki rat is a spontaneous animal model of non-insulin dependent diabetes mellitus (type 2 diabetes) without obesity (Goto et al., 1988). This model was produced by repeated selective breeding between glucose intolerant rats from a nondiabetic Wistar Kyoto colony (Goto et al., 1988), and has enabled us to study any differences in TRPM5 between wild-type Wistar Kyoto rats and Goto Kakizaki rats.

3.1. WK AND GK RAT ß-CELLS EXHIBIT CA^{2+}-ACTIVATED TRPM5-LIKE CURRENT

Pancreatic exocrine tissue digestion from Wistar Kyoto and Goto Kakizaki was initiated with intraductal perfusion of 0.25 mg/ml collagenase type xi (Sigma catalog number C7657) in 0.5% Albumin, Bovine Serum, Fraction V (Calbiochem catalog number 12659) in Hanks Balanced Salt Solution (Media Tech catalog number MT21023CV). Islets were then individually hand picked. Following digestion with 0.25% Trypsin-EDTA (Sigma catalog number T4049), islet ß-cells were subseqeuntly plated on polylysine (Sigma catalog number P8920) coated coverslips and allowed to recover in RPMI-1640 (Media Tech catalog number MT 10043CV) containing 10% Fetal Bovine Serum (Invitrogen catalog number 16140071) in 37ºC in a 5% CO_2 humidified incubator overnight. In this set of experiments, cells were bathed in normal sodium ringer (140 mM NaCl (Sigma catalog number S9888), 2.8 mM KCl (Sigma catalog number

P9333), 2 mM $MgCl_2$ (Sigma catalog number M1028) and 10 mM Hepes-NaOH (Sigma catalog number H3375 and Fisher catalog number SS255-1) solution that contained 4 mM glucose (Sigma catalog number G8270), 10 mM CsCl (Fisher catalog number BP210) and 1 mM $CaCl_2$ and perfused with a cesium-based glutamate (comprised of 140 mM L-(+)-glutamic acid (Fisher Scientific catalog number A125) and cesium hydroxide (Sigma catalog number 21351-79)) ringer (8 mM NaCl (Sigma catalog number S9888), 1 mM $MgCl_2$ (Sigma catalog number M1028) and 10 mM Hepes-CsOH (Sigma catalog number H3375 and Sigma catalog number 21351-79) solution. In these sets of experiments cells were held at -40 mV and were subjected to a voltage ramp from -100 mV to +100 mV. Currents were collected at -80 mV and +80 mV. Following whole-cell establishment, cells were exposed to 20 μM ionomycin (Sigma catalog number I0634) in Ca^{2+}-free sodium ringer solution for 8 seconds. Ionomycin is an electroneutral Ca^{2+} ionophore which exchanges one Ca^{2+} ion for two hydrogen ions. Because ionomycin is lypophyllic, it is easily transported through and incorporated into the plasma membrane and the endoplasmic reticulum of cells. When coupled with Ca^{2+}-free sodium ringer solution, ionomycin effects on the endoplasmic reticulum can be measured. The endoplasmic reticulum is the Ca^{2+} storage organelle of cells. Upon external exposure of the cell to ionomycin, the stored Ca^{2+} in the endoplasmic reticulum is released into the cytosol of the cell. It is believed that this Ca^{2+} triggers the activation of TRPM5.

3.1.1. TRPM5 current in rat ß-cells during ionomycin-induced Ca^{2+} mobilization

Figure 1A shows the effect of a brief ionomycin exposure on pancreatic ß-cells. In plotting the currents as a function of time, we extracted the current measured at -80 mV for the inward current and the current measured at +80 mV for the outward current. The measured currents, as illustrated in Figure 1A, were substantially asymmetrical with the outward current being larger than the inward current. With regard to the Wistar Kyoto rat pancreatic ß-cell, the maximum outward current as a result of ionomycin stimulation was 218.90 pA while the maximum inward current measured at 60.29 pA. With regard to the Goto Kakizaki rat pancreatic ß-cell, the maximum outward current was 127.31 pA while the maximum inward current measured at 57.57 pA. These data suggest that pancreatic ß-cells of Wistar Kyoto and Goto Kakizaki rats have ionomycin-induced TRPM5-like current that display typical TRPM5-like behavior with assymetrical current amplitudes. These data also illustrate that Wistar Kyoto and Goto Kakizaki rat pancreatic ß-cells display characteristic TRPM5 transient behavior where the current activation is followed by inactivation of the current within 20 seconds. In addition, these data show that the TRPM5-like current measured at +80 mV is significantly smaller in the Goto Kakizaki rat pancreatic ß-cells when compared to the ß-cells of the Wistar Kyoto rat. The development of a more symmetrical inward to outward ratio current as observed in the Wistar Kyoto current traces is likely due to the activation of TRPM4 which is ubiquitously expressed and very closely related in genetic sequence and structure to TRPM5.

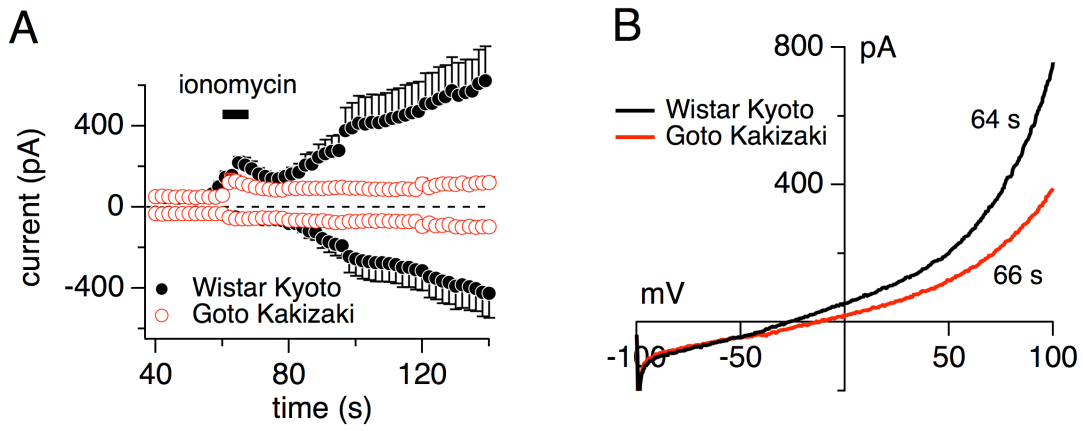

Figure 1. Pancreatic ß-cell response to ionomycin. (A) Wistar Kyoto (●), n=17 and Goto Kakizaki (○), n=23, rat pancreatic ß-cell currents recorded at –80 and +80 millivolts show TRPM5-like characteristics in response to ionomycin stimulation. (B) The current vs. voltage relationship of pancreatic ß-cells isolated from Wistar Kyoto (—) and Goto Kakizaki (—) rat in response to a brief exposure to ionomycin at a specific time point. The I/V relationship shows TRPM5-like characteristics, namely an outward rectification and a transient nature. $p < 0.05$ WK vs. GK outward.

Figure 1B shows the current versus voltage relationship of a single Wistar Kyoto and a single Goto Kakizaki pancreatic ß-cell at a specific time point during ionomycin application, where the TRPM5-like current is activated. With regard to the Wistar Kyoto, the trace was extracted at the 64 second time point. The trace representing the Goto Kakizaki response was extracted at the time point of 66 seconds. Because ionomycin is a Ca^{2+} ionophore, one can assume that the effect of ionomycin on rat pancreatic ß-cells is due to Ca^{2+}. The potential at which the current reverses from being an inward current to being an outward current was -26 mV for the Wistar Kyoto and -14 mV for the Goto Kakizaki rat. Being activated by Ca^{2+}, the outward rectification of the trace and the current's transient nature are distinguishable features of the TRPM5 ion channel. These

data reinforce our hypothesis that rat pancreatic ß-cells possess a TRPM5-like current. These current versus voltage relationships are recordings taken from single cells. Cell size was not accounted for in these data traces and the traces have not been subtracted for background current.

3.1.2. Ionomycin-induced Ca^{2+} signal and TRPM5

Due to the presence of a TRPM5-like current from the Wistar Kyoto and Goto Kakizaki rat pancreatic ß-cells as a result of ionomycin exposure, it was important to measure the Ca^{2+} signal generated from such exposure. In this group of experiments we performed whole-cell patch clamp measurements in conjunction with measuring intracellular calcium levels using the ratitometric Ca^{2+} sensitive fluorescent dye. Cells were perfused with 200 µM Fura-2 (Life Technologies catalog number F1200) solubilized in a cesium-based glutamate (comprised of 140 mM L-(+)-glutamic acid (Fisher Scientific catalog number A125) and cesium hydroxide (Sigma catalog number 21351-79)) ringer (8 mM NaCl (Sigma catalog number S9888), 1 mM $MgCl_2$ (Sigma catalog number M1028) and 10 mM Hepes-CsOH (Sigma catalog number H3375 and Sigma catalog number 21351-79)) solution. Cells were bathed in normal sodium ringer (140 mM NaCl (Sigma catalog number S9888), 2.8 mM KCl (Sigma catalog number P9333), 2 mM $MgCl_2$ (Sigma catalog number M1028) and 10 mM Hepes-NaOH (Sigma catalog number H3375 and Fisher catalog number SS255-1) solution that contained 4 mM glucose (Sigma catalog number G8270), 10 mM CsCl (Fisher catalog number BP210) and 1 mM $CaCl_2$ (Sigma catalog number 4901). In these sets of experiments cells were held at 0 mV and were subjected to a voltage ramp from -100 mV to +100 mV.

Data of current development were collected at -80 mV and +80 mV. Following whole-cell establishment and attainment of a stable baseline intracellular calcium recording, cells were exposed to 20 μM ionomycin in calcium-free sodium ringer solution for 8 seconds.

Figure 2A shows the effect of a brief exposure to ionomycin on the Ca^{2+} stores in pancreatic ß-cells of Wistar Kyoto and Goto Kakizaki rats. This data suggests that Wistar Kyoto and Goto Kakizaki pancreatic ß-cells contain ionomycin-sensitive intracellular Ca^{2+} stores. The rate of release from both rat ß-cell populations are similar. However, the amplitude of release is significantly different between both populations. The Ca^{2+} signal from the Wistar Kyoto pancreatic ß-cells had an estimated maximum Ca^{2+} release amplitude of 4 μM while the Ca^{2+} signal from the Goto-Kakizaki rat exhibited an estimated maximum Ca^{2+} release amplitude of 2 μM. Another noticeable observation is that following ionomycin application, the Goto-Kakizaki rat ß-cells approached basal Ca^{2+} levels faster than ß-cells from the Wistar Kyoto rat.

Figure 2B shows the whole-cell current developments at -80 mV for the inward current and +80 mV for the outward current for both Wistar Kyoto and Goto Kakizaki ß-cells in response to an ionomycin-induced Ca^{2+} signal. These data show the resulting current development from the Ca^{2+} signal generated in Figure 2A. These data have been normalized for cell size. Wistar Kyoto pancreatic ß-cells had a normalized inward current size of 4.74 pA/pF and a normalized outward current size of 32.04 pA/pF. Goto Kakizaki pancreatic ß-cells had a normalized inward current size of 2.54 pA/pF and a normalized outward current size of 18.66 pA/pF. In comparing the electrophysiology data between

Figures 1A and 2B, the noticeable difference is the absence of the secondary response observed in Figure 1A, of the development of the ubiquitous TRPM4 current.

Figure 2C shows the current vs. voltage relationship of a single Wistar Kyoto and a single Goto Kakizaki ß-cell at a specific time point during ionomycin exposure. The trace representing the Wistar Kyoto ß-cell was extracted at 88 seconds and the trace representing the Goto Kakizaki ß-cell was extracted at 70 seconds. The potential at which the current reverses from an inward current to an outward current remained relatively constant in both cells when compared with the reversal potential in Figure 1B. The reversal potential for the Wistar Kyoto pancreatic ß-cell was -29 mV while the reversal potential for the Goto-Kakizaki pancreatic ß-cell -15 mV. These current vs. voltage relationship data almost mirror current vs. voltage relationship in Figure 1B. Thus, these data reinforce our hypothesis that rat pancreatic ß-cells possess a TRPM5-like current. These current versus voltage relationships were obtained from single cell recordings. Cell size was not considered in these data traces and the traces have not been subtracted for background current.

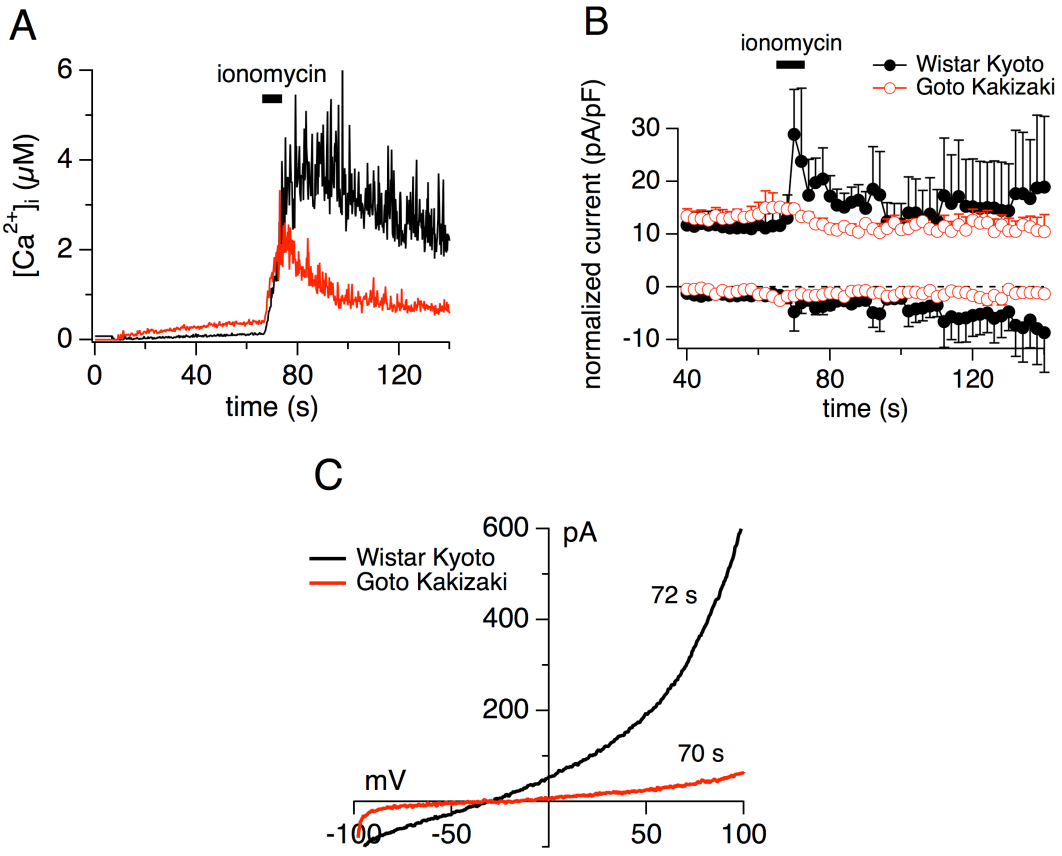

Figure 2. Wistar Kyoto and Goto Kakizaki rat pancreatic ß-cell Ca^{2+} response to ionomycin. Extracellular exposure to ionomycin elicits Ca^{2+} release in Wistar Kyoto (–), n=3 and Goto Kakizaki (–), n=3 rat pancreatic ß-cells (A). An increase in intracellular Ca^{2+} leads to the activation of TPRM5-like current in pancreatic ß-cells of Wistar Kyoto (●), n=3 and Goto Kakizaki (○), n=3 rat pancreatic ß-cells. Current measured at -80 mV and +80 mV(B). The current vs. voltage relationship of pancreatic ß-cells isolated from Wistar Kyoto (–) and Goto Kakizaki (–) rat in response to a brief exposure to ionomycin at a specific time point. The I/V relationship shows TRPM5-like characteristics, namely an outward rectification and its transient behavior. $p < 0.05$ WK vs. GK outward.

3.2. SURFACE STRUCTURE OF VIABLE WISTAR KYOTO AND GOTO KAKIZAKI RAT PANCREATIC ß-CELLS ARE RECOGNIZED BY THE MONOCLONAL ANTIBODY K14D10. TRPM5 IS ALSO SHOWN TO BE DIFFERENTIALLY EXPRESSED.

In order to ascertain the expression level of TRPM5 in rat pancreatic ß-cells and to determine the viability of the isolated cells, we incorporated double immunostaining. We utilized K14D10 (Enzo Life Sciences, catalog number ALX-803-052-C100) antibody to bind the surface structure of viable rat pancreatic ß-cells. K14D10 antibody is highly specific to viable rat pancreatic ß-cells. We also incorporated the use of a TRPM5-specific antibody (generously donated by Robert F. Margolskee). In this set of experiments, freshly isolated (<16 hr) pancreatic ß-cells were subjected to 2% paraformaldehyde cellular fixation followed by a subsequent 2% BSA block. Cells were then incubated with the ß-cell surface-specific monoclonal antibody K14D10. Beta cells were then permeablelized with 0.2% triton X-100 and reblocked with 2% BSA. To examine whether ß-cells expressed TRPM5, the cells were incubated in antibody against TRPM5. In order to label the cells and determine the specificity of the two primary antibodies for viable rat pancreatic ß-cells and TRPM5, the pancreatic ß-cells were secondarily exposed to the fluorophores Alexa Fluor 568 (anti-mouse) (Invitrogen, catalog number, A11031) for K14D10 binding and Alexa Fluor 488 (anti-rabbit) (Invitrogen, catalog number, A11034) for TRPM5 expression. Finally, fixed and stained cells were mounted on glass slides using ProLong Gold Antifade Reagent with DAPI (Invitrogen, catalog number, P-36931). DAPI staining is important to show intact DNA, which would indicate cell condition prior to fixing and staining. Spleen cells obtained from Wistar Kyoto rat were used as negative controls. Images were obtained using a

Zeiss LSM 5 Pascal Confocal Microscope (RCUH-Core Facility). Pancreatic ß-cells from Wistar Kyoto rats and Goto Kakizaki rats were cultured in growth media containing 4 mM glucose for 16 hours. A concentration of 4 mM glucose is equivalent to blood glucose levels of around 70 mg/dl which is the fasting blood glucose level of healthy individuals. With the K14D10 antibody (red) recognizing the surface structure of viable rat pancreatic ß-cells and the TRPM5 antibody (green) recognizing TRPM5, we are able to determine if the Wistar Kyoto and Goto Kakizaki pancreatic ß-cells are both viable after isolation and if they express the TRPM5 channel.

3.2.1. Co-immunostaining of WK and GK rat pancreatic ß-cells

Figure 3A shows the exposure of Wistar Kyoto pancreatic ß-cells to both the K14D10 and the TRPM5 antibodies. Figure 3A clearly shows that the cells isolated from the Wistar Kyoto pancreas are indeed pancreatic ß-cells. The K14D10 detection in these pancreatic ß-cells is also an indication that these cells are viable, thereby validating that any future experiments performed on these cells within 16 hours of isolation were fit cells. In addition, Figure 3A shows that TRPM5 is present in Wistar Kyoto pancreatic ß-cells. While the TRPM5 protein is detected, it is unclear of its distribution. The distribution of TRPM5 appears to be sparsely localized to the membrane but distributed more randomly and throughout the cell.

Figure 3B also clearly shows that the cells isolated from the Goto Kakizaki pancreas are also viable pancreatic ß-cells. While the pancreatic ß-cells of the Goto Kakizaki rat were exposed to the TRPM5 antibody, there was no detection of the TRPM5 channel, as shown in Figure 3B.

Images from Figures 3A and 3B were obtained from the pancreatic ß-cells harvested on the same day and cultured and treated in an identical fashion. While nuclei staining with DAPI was included in this protocol, we did not include that stain on this figure because the K14D10 antibody was sufficient to illustrate cell viability prior to cell fixation.

A

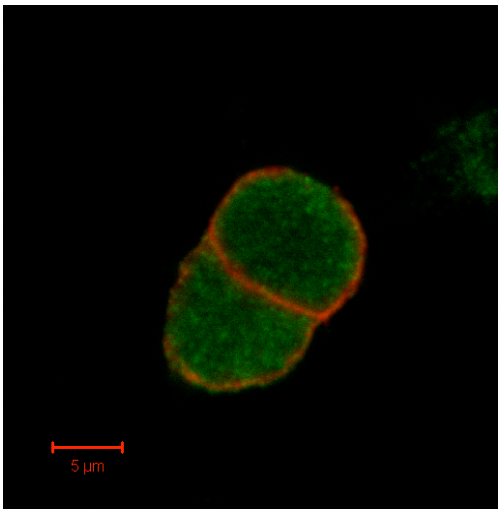

Figure 3A. Co-immunostaining data in Wistar Kyoto pancreatic ß-cells. K14D10 (red) and anti-TRPM5 (green) antibodies were used to identify viable ß-cells and TRPM5 expression, respectively, in Wistar Kyoto rat pancreatic ß-cells.

B

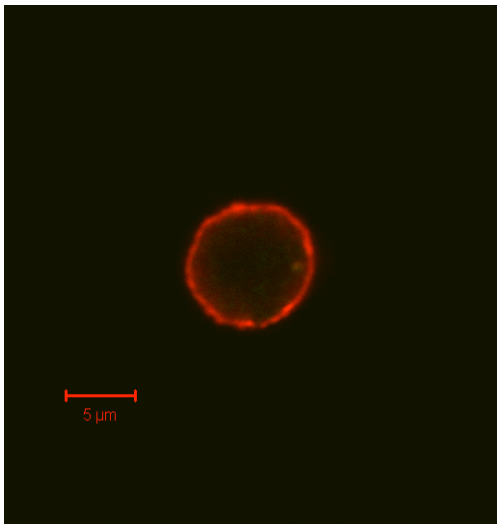

Figure 3B. Co-immunostaining data in Goto Kakizaki pancreatic ß-cells. K14D10 (red) and anti-TRPM5 (green) antibodies were used to identify ß-cells and TRPM5 expression, respectively, in Goto Kakizaki rat pancreatic ß-cells.

3.2.2. Exposure to 10 mM glucose and co-immunostaining of rat pancreatic ß-cells

In order to study the effects of high glucose on TRPM5 expression and rat pancreatic ß-cell viability in Wistar Kyoto, we incorporated the same immunostaining protocol as above. Prior to staining, we incubated the cells in growth media containing 10 mM glucose for at least 16 hours.

As previously mentioned, prior to fixing and staining, Wistar Kyoto rat pancreatic ß-cells were cultured in media containing 10 mM glucose for 16 hours. We used 10 mM to mimic chronic hyperglycemia in vitro. Because chronic hyperglycemia is a classic sign of type-2 diabetes, because the Goto Kakizaki rat is a type-2 diabetes model and because the Goto Kakizaki rat did not show any detectable TRPM5 via antibody staining, we decided to examine the effects of a 16-hour exposure to 10 mM glucose (hyperglycemic condition) on the Wistar Kyoto rat pancreatic ß-cell. Figure 4 illustrates that K14D10 antibody (red) recognized the pancreatic ß-cells of the Wistar Kyoto rat and that those cells remained viable under the stress of a high glucose environment. However, this 16 hour incubation of Wistar Kyoto ß-cells in 10 mM glucose resulted in an reduction of TRPM5 (green) expression. These data were collected on the same day as the data collected in Figure 3. Therefore, the positive control for this experiment is the Wistar Kyoto data in Figure 3A. While the DAPI stain was included in this protocol, we did not include it in this figure because the K14D10 antibody is sufficient to show cell viability prior to cell fixation.

Figure 4. Wistar Kyoto rat pancreatic ß-cells exhibit a reduction in TRPM5 expression after a 16-hour exposure to 10 mM glucose grwoth media. Pancreatic ß-cells from Wistar Kyoto rat were subjected to a double-staining protocol to examine the effects of a high glucose environment on TRPM5 expression. While K14D10 staining shows viable pancreatic ß-cells, the absence of TRPM5 staining shows a noticeable reduction in TRPM5 expression is noticeably reduced in viable rat pancreatic ß-cells after a 16 hour exposure to high glucose media.

3.2.3. Assessing antibody specificity using rat spleen cells

To ascertain the specificity of both antibodies, spleen cells were isolated from Wistar Kyoto rat and subjected to the same fixation and staining protocol as described above. Figure 5 shows the results of the double staining protocol on Wistar Kyoto rat spleen cells. The only detectable stain came from the DNA-specific DAPI stain from the ProLong Gold, which was very localized to the nucleus thereby indicating normal, healthy cell conditions prior to staining. Figure 5 also re-affirms the specificity of K14D10 as a pancreatic ß-cell marker because there was no detectable emission that would be expected if K14D10 was non-specific. In addition, specificity of the TRPM5 antibody from Robert F. Margolskee was also reaffirmed in this case due to no measurable emission one would expect if the antibody was non-specific. TRPM5 has approximately 40% structural homology with TRPM4, a close relative of TRPM5 that is also a Ca^{2+}-activated, non-specific monovalent cation channel. This homology has been

problematic in finding an antibody that is specific to TRPM5. With TRPM4 being ubiquitously expressed and with TRPM4 sharing close structural homology with TRPM5, it would be difficult to conclude that the flourescence we observe in the pancreatic ß-cells is exclusively due to TRPM5 expression. However, since TRPM4 has been shown to be expressed in spleen cells and being that spleen cells do not express TRPM5, it can be verified that the Margolskee antibody is indeed specific to TRPM5.

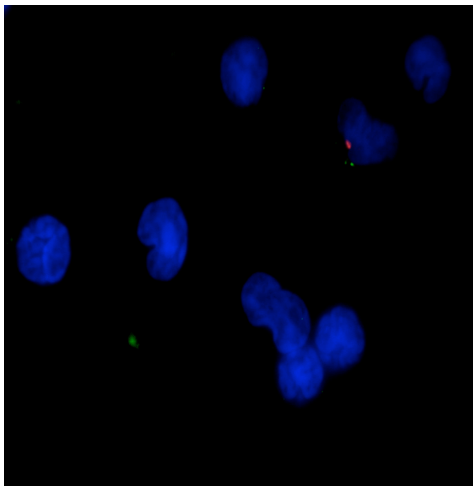

Figure 5. Wistar Kyoto rat spleen cells are used to determine antibody specificity toward K14D10 and TRPM5. Spleen cells from Wistar Kyoto rat were subjected to a double-staining protocol to determine whether the antibodies incorporated in this study were specific for K14D10 cell surface and TRPM5 expression.

3.3. GLUCOSE STIMULATION AND THE CA^{2+} RESPONSE IN WK AND GK PANCREATIC ß-CELLS.

Pancreatic ß-cells were isolated from Wistar Kyoto and Goto Kakizaki rats and cultured at 37ºC in a 5% CO_2 humidified incubator overnight in growth media (RPMI-1640 (Media Tech catalog number MT 10043CV) containing 10% Fetal Bovine Serum (Invitrogen catalog number 16140071) containing either 4 mM or 10 mM glucose. The cells were subsequently bathed in sodium-based ringer solution (140 mM NaCl (Sigma catalog number S9888), 2.8 mM KCl (Sigma catalog number P9333), 2 mM $MgCl_2$

(Sigma catalog number M1028) and 10 mM Hepes-NaOH (Sigma catalog number H3375 and Fisher catalog number SS255-1) which contained 5 μM Fura-2 AM (Invitrogen catalog number, F-1221) and 1 mM $CaCl_2$ (Sigma catalog number 4901). Cells were then incubated for 30 minutes to allow for fura loading. After fura loading was complete, cells were subjected to Ca^{2+} measurement data acquisition and allowed to attain stable Ca^{2+} baseline. When a stable and steady Ca^{2+} baseline was observed, pancreatic ß-cells were extracellularly exposed to 16.7 mM glucose, a concentration shown to stimulate insulin secretion (D'Ambra et al., 1990), in Ca^{2+}-free extracellular media for five minutes. Intracellular calcium was measured using Tillvision 4.0. The data is reported as a ratio of excitation between 340 and 380 nm. In these sets of experiments, cells were subjected to 16.7 mM glucose and normal saline exposure to examine the effects of a stimulatory glucose concentration on Ca^{2+} signaling in pancreatic rat pancreatic ß-cells.

3.3.1. The glucose-stimulated Ca^{2+} response of Wistar Kyoto rat pancreatic ß-cells

Figure 6A shows the ratiometric Ca^{2+} response of Wistar Kyoto rat pancreatic ß-cells cultured overnight in media containing 4 mM glucose. This figure shows the effect of 16.7 mM glucose exposure on the Ca^{2+} response of Wistar Kyoto rat pancreatic ß-cells under normal growth (4 mM glucose) conditions. Cells that were exposed to 16.7 mM glucose show a maximum Ca^{2+} ratiometric signal of 544.10 while the cells exposed to saline (control) maintained a steady and stable baseline, an indication of that the responses we observe were legitimate.

Figure 6B shows the ratiometric calcium response of Wistar Kyoto rat pancreatic ß-cells cultured overnight in growth media containing 10 mM glucose. As mentioned earlier, culturing cells in growth media containing 10 mM glucose is equivalent to hyperglycemic conditions exihibited in diabetes. Figure 6B shows that the control group and the experimental group are indistinguishable, where the maximum Ca^{2+} ratio for the control group (saline) was 591.15 while the maximum ratio for the experimental group (16.7 mM glucose) was 555.83. The fact that the saline treatment responded with an increase in Ca^{2+}, where no Ca^{2+} response is expected, shows that the overnight treatment of 10 mM glucose perturbed the Ca^{2+} dynamic of the control cells. If a 10 mM glucose overnight incubation had no effect on cellular function, then the saline group would respond similarly to the saline group shown in the 4 mM glucose treated cells as observed in figure 6A.

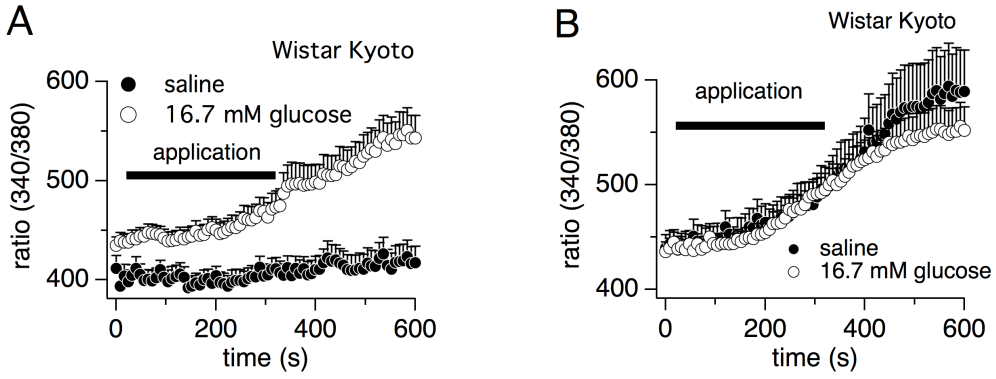

Figure 6. Wistar Kyoto rat pancreatic ß-cell Ca^{2+} response to stimulatory concentration of glucose when cultured overnight in 4 mM and 10 mM glucose. (A) Wistar Kyoto pancreatic ß-cells grown in 4 mM overnight were exposed to a stimulatory concentration of glucose (○), n=21 and normal saline (●), n=37. The traces show the ratiometric Ca^{2+} signal as a result of this exposure. Cells that were exposed to 16.7 mM glucose show a maximum Ca^{2+} ratiometric signal of 544.10 while the cells exposed to saline only (control) remained steady and stable. $p < 0.01$.

(B) Pancreatic ß-cells grown overnight in media containing 10 mM glucose were exposed to a stimulatory concentration of glucose. The traces show the ratiometric Ca^{2+} signal as a result of this exposure. The responses of the saline (●)treatment (n=27) and the 16.7 mM glucose (○) treatment (n=45) are nearly indistinguishable with maximum ratiometric Ca^{2+} responses of 591.15 and 555.83, respectively.

3.3.2. The glucose-stimulated Ca^{2+} response of Goto Kakizaki rat ß-cells

Figure 7A shows the ratiometric Ca^{2+} response of Goto Kakizaki rat pancreatic ß-cells to a stimulatory concentration of glucose (16.7 mM). Prior to stimulation with 16.7 mM glucose, this population of cells was subjected to an overnight incubation in growth media containing 4 mM glucose. Goto Kakizaki rat pancreatic ß-cells that were exposed to normal saline solution exhibited a higher-than-normal Ca^{2+} ratio baseline of 493.32. In addition, during the saline solution application, the Goto Kakizaki rat pancreatic ß-cells responded with an unexpected increase in the ratiometric Ca^{2+} response reaching a maximum of 599.92. The Goto Kakizaki rat pancreatic ß-cells that were exposed to 16.7 mM glucose began with a Ca^{2+} baseline of 412.33. During and following 16.7 mM glucose exposure, these cells did not produce any significant response, having a maximum ratiometric Ca^{2+} response at 476.71.

Figure 7B illustrates the effect of growth media containing 10 mM glucose on the Ca^{2+} signal in Goto Kakizaki rat pancreatic ß-cells in response to 16.7 mM glucose stimulation. Prior to stimulation with 16.7 mM glucose, the Goto Kakizaki rat pancreatic ß-cells were cultured in growth media containing 10 mM glucose for at least 16 hours. We used 10 mM to mimic chronic hyperglycemia in vitro. Because chronic hyperglycemia is a classic sign of type-2 diabetes and because the Goto-Kakizaki rat is a

type 2 diabetes model the 10 mM glucose environment could be considered the "normal" environment for these cells. Figure 7B shows the Ca^{2+} response of Goto Kakizaki rat pancreatic ß-cells to 16.7 mM stimulation with glucose when cultured under hyperglycemic conditions. The fact that the pancratic ß-cells that were exposed to the saline treatment remained very close to baseline indicates that the cells were stable prior to and during the experiment. The response of the cells to 16.7 mM glucose stimulation was very significant reaching a maximum Ca^{2+} ratio of 884.22. The Ca^{2+} baseline was somewhat higher than that of the Wistar Kyoto however, that has no bearing on the pronounced response.

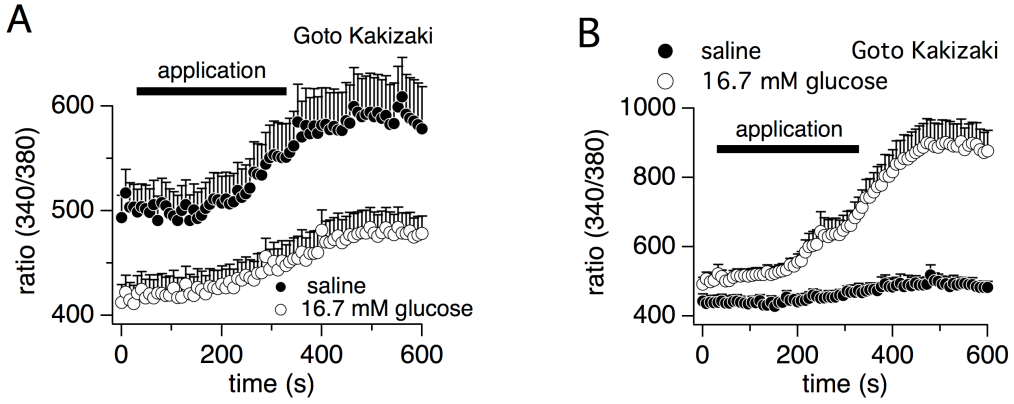

Figure 7. Goto Kakizaki rat pancreatic ß-cell Ca^{2+} response to stimulatory concentration of glucose when cultured overnight in 4 mM glucose and 10 mM glucose. (A) Pancreatic ß-cells grown overnight in growth media containing 4 mM glucose were exposed to normal saline (●), solution (n=10) and a stimulatory concentration of glucose (○), n=11. The traces show the ratiometric Ca^{2+} signal as a result of this treatment. $p < 0.01$. The pancreatic ß-cells, under growth conditions of 4 mM glucose and 16.7 mM glucose treatment produced a slight increase in the ratiometric Ca^{2+} signal. (B) Pancreatic ß-cells grown overnight in growth media containing 10 mM glucose were exposed to normal saline (●) solution (n=6) and a stimulatory concentration of glucose (○), n=14. The traces show the ratiometric Ca^{2+} signal as a result of this treatment with a maximum ratio of 884.22 in cells incubated overnight in 10 mM glucose and subsequently stimulated with 16.7 mM glucose. $p < 0.01$.

3.4. THE CARBACHOL-INDUCED CA^{2+} RESPONSE AND TRPM5 ACTIVATION IN WK AND GK PANCREATIC ß-CELLS.

In order to measure intracellular Ca^{2+} and the TRPM5-like current in a more physiological context, we utilized carbamoylcholine chloride (carbachol) (Sigma Aldrich catalog number C4382) on pancreatic ß-cells of both Wistar Kyoto and Goto Kakizaki rats to elicit a Ca^{2+} response. Carbachol is a cholinergic agonist which binds to the m3 muscarinic receptor endogenously expressed in the rat pancreatic ß-cell. Here, we employed the whole-cell configuration of the patch-clamp technique in conjunction with Fura-2 Ca^{2+} measurements. Freshly isolated pancreatic ß-cells from Wistar Kyoto and Goto Kakizaki rats were bathed in a sodium-based ringer solution (140 mM NaCl (Sigma Aldrich catalog number S9888), 2.8 mM KCl (Sigma Aldrich catalog number P9333), 2 mM $MgCl_2$ (Sigma Aldrich catalog number M1028) and 10 mM Hepes-NaOH (Sigma Aldrich catalog number H3375 and Fisher catalog number SS255-1) with 1 mM $CaCl_2$ (Sigma catalog number 4901). They were subsequently perfused with 200 µM Fura-2 (Life Technologies catalog number F1200) solubilized in a cesium-based glutamate (comprised of 140 mM L-(+)-glutamic acid (Fisher Scientific catalog number A125) and cesium hydroxide (Sigma Aldrich catalog number 21351-79)) ringer which contained, 8 mM NaCl (Sigma Aldrich catalog number 5886), 1 mM $MgCl_2$ (Sigma Aldrich catalog number M1028) and 4 mM Glucose (Sigma Aldrich catalog number G8270).

The endocrine pancreas receives rich input from sympathetic and parasympathetic nerves (Ahren, 2000; Brunicardi et al., 1987). Aside from glucose, other physiological agents such as neurotransmitters also influence insulin secretion. In addition, rat pancreatic islets have been shown to express m1 and m3 muscarinic receptors (Iismaa et

al., 2000). While both receptors are expressed in equal amounts in pancreatic ß-cells (Iismaa et al., 2000), the m3 receptor subtype is believed to be involved in the parasympathetic regulation of insulin secretion (Boschero et al., 1995; Verspohl et al., 1990). Carbamylcholine (carbachol or cch) is an agent that mimics the parasympathetic neurotransmitter acetylcholine and binds to both m1 and m3 muscarinic receptors (Iismaa et al., 2000). Interaction of carbachol with the m3 muscarinic receptor leads to activation of phospholipase C, the subsequent generation of inositol 1,4,5-triphosphate and diacylglycerol and finally the mobilization of Ca^{2+} from intracellular Ca^{2+} stores.

In these sets of experiments cells were held at 0 mV and were subjected to a voltage ramp from -100 mV to +100 mV. Data from any current development were collected at -80 mV and +80 mV. Following whole-cell establishment and once the calcium baseline was established, pancreatic ß-cells were given brief exposure to 100 μM carbachol in filtered Ca^{2+}-free sodium ringer solution (140 mM NaCl (Sigma Aldrich catalog number S9888), 2.8 mM KCl (Sigma Aldrich catalog number P9333), 2 mM $MgCl_2$ (Sigma Aldrich catalog number M1028) and 10 mM Hepes-NaOH (Sigma Aldrich catalog number H3375 and Fisher catalog number SS255-1).

3.4.1. The carbachol-induced Ca^{2+} response of WK and GK rat pancreatic ß-cells

Figure 8A shows the effect of 100 μM carbachol on pancreatic ß-cells of both Wistar Kyoto and Goto Kakizaki rats. Because the stimulation was done in the absence of extracellular Ca^{2+}, the initial Ca^{2+} signal is due to Ca^{2+} release from intracellular Ca^{2+} storage organelles like the endoplasmic reticulum. The Ca^{2+} response of the pancreatic ß-cells from both populations is very typical and also appear relatively similar to each

other. The Ca^{2+} response from both populations of ß-cells to carbachol stimulation was characteristically fast. The maximal response from both populations of cells was followed by a fast decrease with a return of the Ca^{2+} to basal levels. Pancreatic ß-cells from Wistar Kyoto had a response that reached a maximum intracellular Ca^{2+} concentration of 457 nM while pancreatic ß-cells from Goto Kakizaki rat had a response that reached a maximum intracellular Ca^{2+} concentration of 434 nM.

3.4.2. The carbachol-induced Ca^{2+} signal activates TRPM5 in rat pancreatic ß-cells

The exposure of Wistar Kyoto and Goto Kakizaki rat pancreatic ß-cells to carbachol elicited a sufficient Ca^{2+} signal in both ß-cell types. This very characteristic Ca^{2+} signal resulted in the TRPM5-like current development in ß-cells from pancreatic Wistar Kyoto and Goto Kakizaki rats. Figure 8B summarizes the TRPM5-like current development as a result of an intracellular rise in Ca^{2+}, due to agonist stimulation. Figure 8B clearly shows a difference in magnitude between the inward and outward TRPM5-like currents of the Wistar Kyoto pancreatic ß-cells as opposed to the inward and outward currents of the Goto Kakizaki pancreatic ß-cells. The TRPM5-like normalized outward current measured from the Wistar Kyoto pancreatic ß-cells was 8.15 pA/pF while the normalized outward current measured from the Goto Kakizaki pancreatic ß-cells was 4.21 pA/pF. In addition, the normalized inward current measured from the Wistar Kyoto pancreatic ß-cells was -1.51 pA/pF while the normalized inward current measured from the Goto Kakizaki pancreatic ß-cells was -0.43 pA/pF. These data clearly show that the TRPM5-like current observed in the Goto Kakizaki pancreatic ß-cells is significantly

reduced compared to the currents observed in the Wistar Kyoto pancreatic ß-cells, even while the Ca^{2+} signals from both types of pancreatic ß-cells display nearly identical recordings.

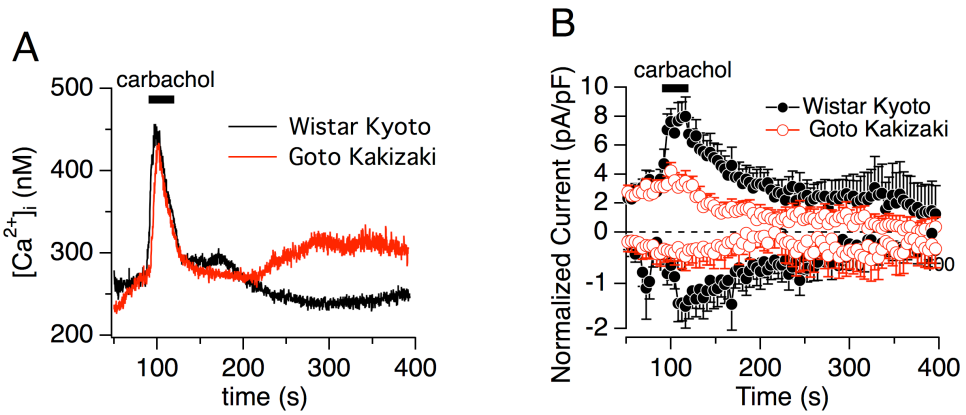

Figure 8. Pancreatic ß-cell Ca^{2+} response to carbachol stimulation and subsequent TRPM5-like current development in Wistar Kyoto and Goto Kakizaki rat pancreatic ß-cells. Pancreatic ß-cells grown in 4 mM overnight were exposed to 100 µM carbachol. (A) The traces show the nanomolar Ca^{2+} signal as a result of this exposure. The Wistar Kyoto (–), n=20 rat responded with a maximum Ca^{2+} signal of 457 nM while the Goto Kakizaki (–), n=28 rat responded with a maximum signal of 434 nM. (B) An increase in intracellular Ca^{2+} due to exposure to 100 µM carbachol elicits a TRPM5-like current response in pancreatic ß-cells of Wistar Kyoto (●), n=20 and Goto Kakizaki (○), n=28 rats. Currents were measured at -80 mV and +80 mV. $p < 0.01$ WK vs. GK outward.

3.4.3. The current vs. voltage relationship of TRPM5 during the carbachol application

The current vs. voltage relationships of the TRPM5-like current in Wistar Kyoto rat pancreatic ß-cell prior to carbachol stimulation (20 seconds) and after carbachol stimulation (136 seconds) are shown in figure 9A. This figure shows a significant activation in the TRPM5-like current (at 136 seconds) with its characteristic outward rectification as exhibited with the increase in inward current during carbachol stimulation

from -14 pA to -71 pA and outward current showing an even greater change in current size with an increase from 52 pA to 190 pA. In addition, the reversal potential shifts from -52.29 mV prior to carbachol stimulation to a reversal potential of -7.81 mV, during activation of the TRPM5-like current. These data reinforce the idea that an increase in intracellular Ca^{2+} leads to activation of a TRPM5-like current in rat pancreatic ß-cells. These current versus voltage relationships are single recordings that have been measured from the same cell. Cell size was not accounted for in these data traces and the traces have not been subtracted for background current.

Figure 9B illustrates the current vs. voltage relationships of TRPM5 in Goto Kakizaki rat pancreatic ß-cell prior to carbachol stimulation (24 seconds) and during carbachol stimulation (100 seconds). While the Ca^{2+} signal generated from carbachol stimulation was comparable to the Ca^{2+} signal of Wistar Kyoto rat pancreatic ß-cells, figure 9B shows no significant activation of the TRPM5 current during (100 seconds) or after carbachol stimulation. The 100 second time point was chosen because it exhibited the largest change in current for this individual cell. These current versus voltage relationships are single recordings that have been measured from the from the same cell. The potential at which the current reverses was -45.48 mV prior to carbachol stimulation. The reversal potential in the Goto Kakizaki rat pancreatic ß-cell slightly shifted positive following carbachol stimulation to -32.65 mV. Cell size was not accounted for in these data traces and the traces have not been subtracted for background current.

Figure 9C illustrates the current versus voltage relationship of pancreatic ß-cells from both Wistar Kyoto and Goto Kakizaki rats. This figure highlights the significant difference in response between the pancreatic ß-cells taken from Wistar Kyoto rats as

opposed to Goto Kakizaki rats. While the Ca^{2+} signal from both cell types were comparable with respect to their response to the same stimulus, a TRPM5-like current developed in the Wistar Kyoto pancreatic ß-cells but there was no current development in the Goto Kakizaki pancreatic ß-cells.

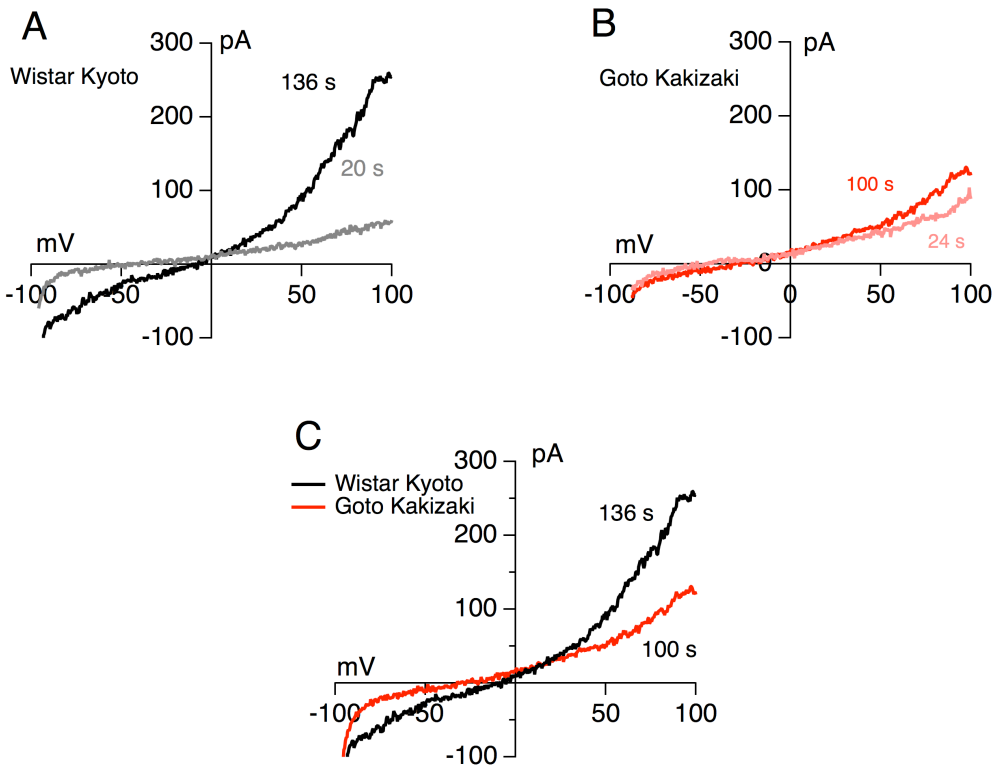

Figure 9. Wistar Kyoto and Goto Kakizaki rat pancreatic ß-cell TRPM5-like current versus voltage relationship in response to extracellular carbachol stimulation. (A) Wistar Kyoto pancreatic ß-cells grown in 4 mM overnight were exposed to 100 µM carbachol. An increase in intracellular Ca^{2+} due to exposure to 100 uM carbachol elicits a TRPM5-like current response in pancreatic ß-cells of Wistar Kyoto. The traces illustrate the current versus voltage relationship measured from a single cell at time points prior to (20 seconds, –) and following (136 seconds, –) carbachol stimulation. On the other hand, with regard to the Goto Kakizaki rat (B), an increase in intracellular Ca^{2+} due to exposure to 100 uM carbachol does not elicit a current response in pancreatic ß-cells of Goto Kakizaki rat. The traces illustrate the current versus voltage relationship measured from a single cell at time points prior to (24 seconds, –) and during (100 seconds, –) carbachol stimulation. Panel C compares the I/V traces of both populations during activation (Goto Kakizaki (–) and Wistar Kyoto (–)) to illustrate the significant difference in TRPM5 response between the two populations of cells.

3.5. CA^{2+} DOSE RESPONSE OF TRPM5 IN WK AND GK PANCREATIC ß-CELLS.

In order to determine the calcium concentration range in which the TRPM5-like current responds, we performed experiments measuring the current size in response to various concentrations of free intracellular Ca^{2+}. Cells were isolated from male rats using the aforementioned protocol. They were cultured overnight in media containing 4 mM glucose. Cells were bathed in normal sodium-based ringer solution (140 mM NaCl (Sigma Aldrich catalog number S9888), 2.8 mM KCl (Sigma Aldrich catalog number P9333), 2 mM $MgCl_2$ (Sigma Aldrich catalog number M1028) and 10 mM Hepes-NaOH (Sigma Aldrich catalog number H3375 and Fisher catalog number SS255-1) with 1 mM $CaCl_2$ (Sigma catalog number 4901). Cells were perfused with cesium-based glutamate (comprised of 140 mM L-(+)-glutamic acid (Fisher Scientific catalog number A125) and cesium hydroxide (Sigma catalog number 21351-79)) ringer (8 mM NaCl (Sigma catalog number S9888), 1 mM $MgCl_2$ (Sigma catalog number M1028) and 10 mM Hepes-CsOH (Sigma catalog number H3375 and Sigma catalog number 21351-79)) solution with 10 mM 5,5'-Dibromo BAPTA (Invitrogen catalog number, D1211) and various concentrations of free cytosolic $CaCl_2$. The on-line WEBMAXC STANDARD program was utilized in calculating free Ca^{2+} values. The whole cell configuration of the patch clamp technique was utilized in determining the effects of various concentrations of free intracellular calcium on TRPM5 in pancreatic ß-cells. In these sets of experiments cells were held at -40 mV and were subjected to a voltage ramp from -100 mV to +100 mV. Currents were collected at -80 mV and +80 mV. The currents measured at +80 mV were utilized in comparing the effects of Ca^{2+} on TRPM5 in pancreatic ß-cells of Wistar Kyoto and Goto Kakizaki rats.

3.5.1. The Ca^{2+} dose response of TRPM5 displays a sigmoidal relationship

Figure 10A shows the calcium dose response curve of TRPM5 in Wistar Kyoto and Goto Kakizaki rat pancreatic ß-cells. Activation of TRPM5 in rat pancreatic ß-cells shows a sigmoidal curve an indication that binding of Ca^{2+} ions to TRPM5 is cooperative. Wistar Kyoto TRPM5 show a I_{max} of 58.64 pA/pF and a K_m of 4.89 μM Ca^{2+} with a Hill coefficient of 2. On the other hand, the pancreatic ß-cells from the Goto Kakizaki rat had a I_{max} of 21.87 pA/pF, with a K_m of 3.84 μM Ca^{2+} and a Hill coefficient of 3. While there was greater than 60% difference between the V_{max} values of both ß-cell types, the K_m values remained relatively comparable. The Hill Coefficient demonstrates an increase from 2 to 3 in the Wistar Kyoto and Goto Kakizaki rats, respectively. The Hill Coefficient measures the cooperativity of binding between Ca^{2+} and the channel (Stryer, 1995). Any Hill Coefficient above one indicates cooperative binding which means that the binding of one Ca^{2+} ion enhances the binding of a second Ca^{2+} ion. The change in the Hill coefficient observed between the Wistar Kyoto and Goto Kakizaki pancreatic ß-cells, had no effect on the maximum current. The TRPM5 current of the Goto Kakizaki pancreatic ß-cells exhibited very significant reductions in its currents across nearly all concentrations of Ca^{2+} compared to the TRPM5 current of the Wistar Kyoto rat pancreatic ß-cells. The sigmoidal fits were obtained using IGOR Pro software version 6.34.

3.5.2. The current vs. voltage relationships of TRPM5 at 6 μM Ca^{2+}

Figure 10B shows the current versus voltage relationship of TRPM5 in pancreatic ß-cells of Wistar Kyoto and Goto Kakizaki rat. We utilized traces from 6 μM Ca^{2+} concentration for both I/V graphs. The I/V trace taken from the Wistar Kyoto rat ß-cell exhibited typical outward rectification with an outward current size of 441 pA and an inward current size of -240 pA. The I/V trace taken from the Goto Kakizaki rat ß-cells also exhibited the typical TRPM5 characteristic of outward rectification, albeit smaller, with its outward current at 316 pA and its inward current at -84 pA. The reversal potential for the trace taken from the Wistar Kyoto rat pancreatic ß-cells occurred at approximately -6 mV, while the reversal potential for the trace taken from the Goto Kakizak rat pancreatic ß-cells occurred at approximately -16 mV.

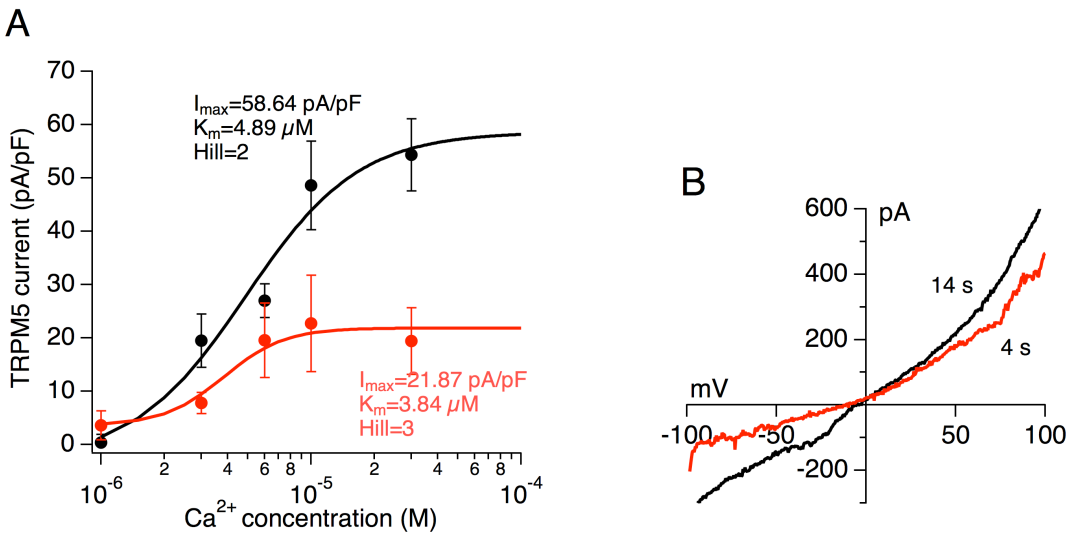

Figure 10. TRPM5 Ca^{2+} dose response curve of Wistar Kyoto and Goto Kakizaki rat pancreatic ß-cells. Wistar Kyoto (●) and Goto Kakizaki (●) pancreatic ß-cells were grown in 4 mM glucose overnight and subsequently perfused with various concentrations of Ca^{2+} during whole cell patch clamp experiments. (A) Wistar Kyoto TRPM5 show a V_{max} of 58.64 pA/pF and a K_m of 4.89 μM Ca^{2+} with a Hill coefficient of 2. On the other hand, the pancreatic ß-cells from the Goto Kakizaki rat had a V_{max} of 21.87 pA/pF, with a K_m of 3.84 μM Ca^{2+} and a Hill coefficient of 3. $p < 0.05$ at 10 and 30 μM Ca^{2+} for WK vs. GK.

(B) The I/V traces taken from the Wistar Kyoto (−) rat ß-cell exhibited typical outward rectification with an outward current size of 441 pA and an inward current size of -240 pA. The I/V trace taken from the Goto Kakizaki (−) rat ß-cells also exhibited the typical TRPM5 characteristic of outward rectification, albeit smaller, with its outward current at 316 pA and its inward current at -84 pA. The reversal potential for the trace taken from the Wistar Kyoto rat pancreatic ß-cells occurred at approximately -6 mV, while the reversal potential for the trace taken from the Goto Kakizak rat pancreatic ß-cells occurred at approximately -16 mV.

3.6. AN INCREASE IN CELL CAPACITANCE IS ASSOCIATED WITH ELEVATED CA^{2+}_{i} AND TRPM5 ACTIVATION.

Due to the cell membrane's phospholipid bilayer and its inherent nature of separating electrical charges, the cell membrane can be characterized as a parallel-plate capacitor. Just as capacitors operate to store energy, the cell membrane's stored energy is exhibited with an inside negative membrane potential of -80 mV. The relative amount of charge that can be stored across the plasma membrane for a given voltage is measured in capacitance which is dependant upon the cross sectional area of the cell membrane. Thus, we use the capacitance to determine the cell size.

Exocytosis is a complex process that is facilitated by Ca^{2+} and involves a collection of proteins (please see Introduction). Exocytosis is the docking and fusion of membrane vesicles with the plasma membrane. This docking and fusion of vesicles increases the surface area of the plasma membrane. The pancreatic ß-cell is a secretory cell which undergoes exocytosis to secrete insulin. It has also been shown that pancreatic ß-cells also undergo Ca^{2+}-dependant exocytosis during ion channel activation (Cheng et

al., 2007). Therefore, we are able to determine exocytotic activity in the pancreatic ß-cell by measuring any changes in capacitance during patch-clamp experiments. The data displayed in this section were obtained during the experiments performed in section 3.5.

3.6.1. Capacitance increase during TRPM5 activation at 6 μM Ca^{2+} in WK ß-cells

Figure 11A displays the capacitance and TRPM5 current density changes in an individual pancreatic ß-cell from Wistar Kyoto rat during intracellular perfusion with 6 μM free Ca^{2+}. Figure 11A shows a 49% increase in capacitance during TRPM5 activation. Wistar Kyoto rat capacitance increased from 8.31 pF at 254 seconds to 12.36 pF at 374 seconds. TRPM5 current density increased in the Wistar Kyoto rat pancreatic ß-cell from a baseline of 5 pA/pF before activation to a maximum current density of 19.958 pA/pF at time 264 seconds. The TRPM5 current exhibited in this Wistar Kyoto pancreatic ß-cell exhibited the characteristic behavior of transient activation. These capacitance changes were consistently measured in cells perfused with free Ca^{2+} concentrations of 3 μM or higher.

3.6.2. Capacitance increase is slight during M5 activation at 6 μM Ca^{2+} in GK ß-cells

Figure 11B displays the activation of TRPM5 current and capacitance changes in an individual pancreatic ß-cell from Goto Kakizaki rat during intracellular perfusion with 6 μM free Ca^{2+}. Figure 11B shows a 6.7% increase in capacitance during TRPM5 activation. Goto Kakizaki rat capacitance increased from 5.97 pF at 34 seconds to 6.37 pF at 118 seconds. TRPM5 current density increased in the Goto Kakizaki rat pancreatic

ß-cell from a baseline of 1.6 pA/pF before activation to a maximum current density of approximately 10 pA/pF at 118 seconds. Although there was TRPM5 current activation, the current was not transient and activation was sustained.

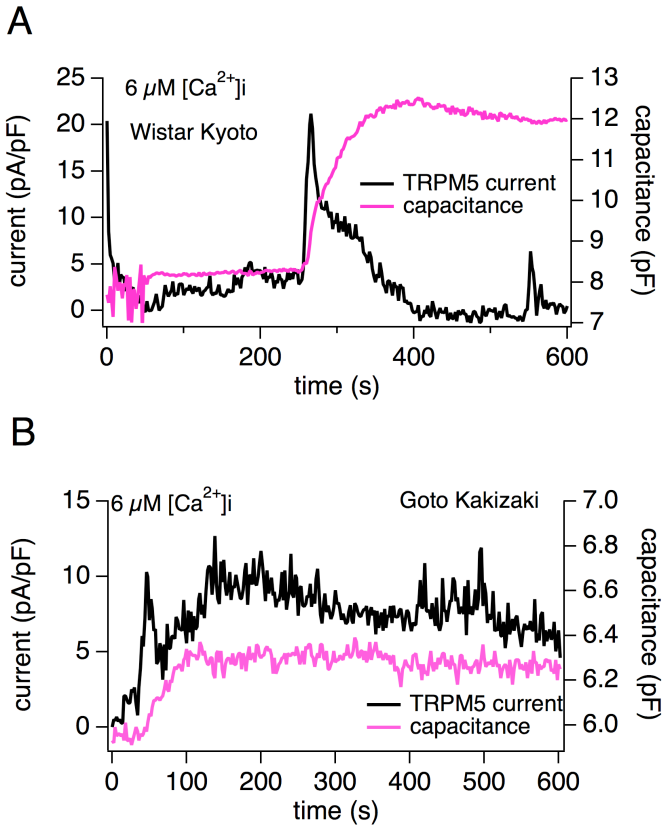

Figure 11. Wistar Kyoto and Goto Kakizaki rat pancreatic ß-cell TRPM5 current density and capacitance increase during intracellular perfusion with 6 μM free Ca^{2+}. (A) Wistar Kyoto TRPM5 current density (−) and capacitance (−) both increase during perfusion with 6 μM Ca^{2+} during whole cell patch clamp experiments. The current density reported here was taken at +80 mV. The current density increased from an average baseline of 5 pA/pF to a maximum of 19.958 pA/pF during activation. Similarly, the capacitance of the Wistar Kyoto pancreatic ß-cell increased by approximately 49% with a capacitance of 8.31 pF prior to activation to a capacitance of 12.36 pF. (B) Goto Kakizaki TRPM5 current density (−) and capacitance (−) both increase during perfusion with 6 μM Ca^{2+} during whole cell patch clamp experiments. The current density reported here was taken at +80 mV. The current density increased from an average baseline of 1.6 pA/pF to a maximum of approximately 10 pA/pF during activation. Similarly, the capacitance of the Goto Kakizaki rat pancreatic ß-cell increased by approximately 6.7% with a capacitance of 5.97 pF prior to activation to a capacitance of 6.37 pF at 118 seconds.

3.7. TRPM5 IS NOT ACTIVATED BY PASSIVE STORE DEPLETION IN RAT PANCREATIC ß-CELLS.

There are conflicting reports regarding TRPM5's activation mechanism (Perez et al., 2002; Prawitt et al., 2003). The contradiction is whether TRPM5 is store-operated or Ca^{2+}-activated. Because there is a possibility that the TRPM5 current in rat pancreatic ß-cells is activated by store depletion, we perfused the cells with 10 mM dibromo-BAPTA to cause passive depletion of the Ca^{2+} stores.

Figure 10 shows no significant activation of an inward current with the development of an outward current through time. The fact that there is no inward current associated with the development of the outward current is a likely indication that the outward current measured is not TRPM5.

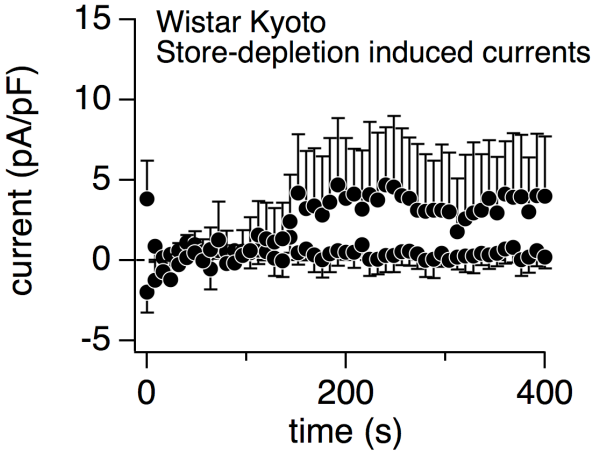

Figure 12. TRPM5 is not activated by store depletion. Wistar Kyoto pancreatic ß-cells were grown in 4 mM glucose overnight and subsequently perfused with a Cs-based ringer containing 10 mM dibromo-BAPTA during whole cell patch clamp experiments. There was no detectable outward or inward current resembling TRPM5 during intracellular perfusion (n=6).

3.8. GLUCOSE-STIMULATED CA^{2+}-SIGNALING IS NOT CONSISTENTLY OBSERVED WHILE PERFORMING PERFORATED-PATCH EXPERIMENTS.

In an attempt to measure the effects of glucose stimulation on intracellular Ca^{2+} signaling of pancreatic ß-cells of Wistar Kyoto rat and draw a connection between glucose stimulation and TRPM5 activation, we employed the use of the perforated-patch technique in conjunction with fura-2 Ca^{2} measurements. In whole-cell patch clamp, the cells are continually perfused with intracellular Ringer's solution which washes out and completely replaces the intracellular contents of the cell. In order to measure the effects of glucose on intracellular Ca^{2+} signaling without disrupting the cell's intracellular contents, we incorporate the use of 80 µM amphotericin B. Amphotericin B is an antibiotic commonly used for fungal infections. It binds to cell membranes and forms transmembrane channels which allow for the movement of monovalent ions such as Na^{+}, K^{+}, H^{+} and Cl^{-}. Therefore, amphotericin B allows for electrical access to the cell without disrupting the intracellular environment of the cell.

The perforated-patch technique was employed to examine the effects of a stimulatory concentration of glucose on the Ca^{2+} response in Wistar Kyoto pancreatic ß-cells. Although the parameters and conditions of the experiment were optimized, the response of the cells to glucose stimulation was disappointing. We performed 48 experiments and of the 48, there were only two cells which responded. As mentitoned previously, single pancreatic ß-cells may behave differently then when they are intact and remain connected with the other cells of the islets. Due to our poor success rate with this experimental protocol, we abandoned this portion of the study. Figures 13A and 13B represent the Ca^{2+}signal and the current responses observed in the only two Wistar Kyoto

cells that responded to stimulation with glucose during the perforated patch experiments. Both figures show the generation of a Ca^{2+} signal(s) and a current response that is associated with the Ca^{2+} signal(s). The current versus voltage relationship of the currents that did develop (figures 13C and 13D) do not represent the TRPM5's signature current versus voltage relationship. It is plausible that the TRPM5 current is in-fact in these traces, however it may be masked with the contaminating non-TRPM5 current, most likely chloride. Therefore, we were unable to draw any conclusions regarding glucose stimulation and TRPM5 activation from these data.

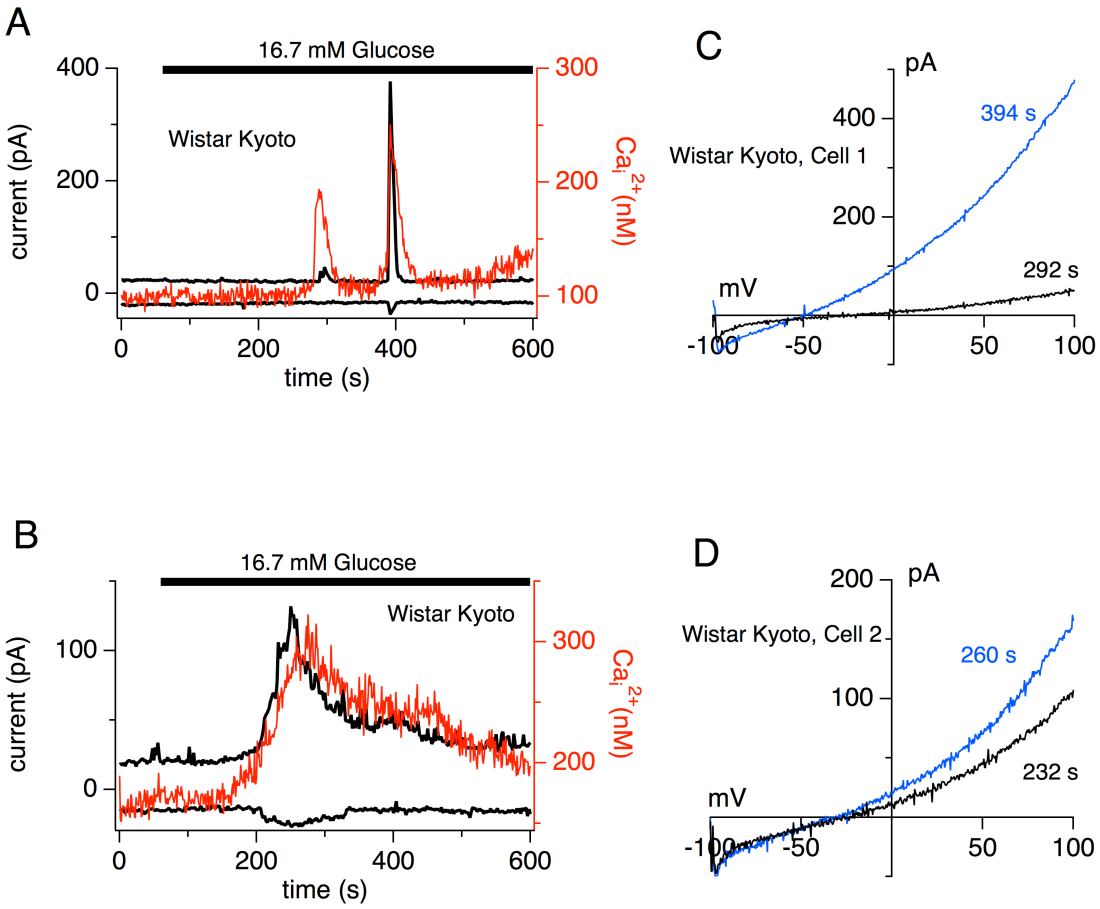

Figure 13. The Ca^{2+} response and subsequent current response of WK pancreatic ß-cells during perforated-patch experiments. Panels A and B represent the response of the only 2 (n=48) individual single cells to glucose stimulation using the perforated patch technique. The Ca^{2+} signals (–) and currents (–) seem to have their responses coincide with each other during glucose stimulation. Upon further analysis of the I/V curves it is apparent that the currents generated in this study are not TRPM5. Panels C and D illustrate the current vs. voltage relationships at 2 different time points of the currents in panels A and B, respectively.

CHAPTER 4. DISCUSSION

We have previously reported the transient receptor potential melastatin subtype 5 (TRPM5) channel to exist in rat pancreatic insulinoma (INS-1) ß-cell line (Prawitt et al., 2003). With the use of whole-cell patch clamp we were able to determine that the INS-1 cell line exhibited several hallmarks of TRPM5 current behavior. More recently it was reported that the TRPM5 channel plays a role in insulin secretion in the Sprague-Dawley rat pancreatic ß-cell (Krishnan et al., 2014). This study focused on TRPM5 in the pancreatic ß-cell of the Wistar Kyoto and the Goto Kakizaki rat. The Goto Kakizaki rat is a Wistar substrain which spontaneously develops type-2 diabetes. We utilized these populations of rats to perform a comparative study of TRPM5 expression and function between the Wistar Kyoto and the Goto-Kakizaki rat pancreatic ß-cells.

4.1. THE IONOMYCIN-INDUCED CA^{2+} SIGNAL AND TRPM5

TRPM5 is a non-selective monovalent cation channel that is activated by Ca^{2+}. Before initiating any comparative study between the normal and the diabetic rats, it was important that we establish the presence of a current that exhibited TRPM5-like characteristics. In order to accomplish this in the most efficient manner, ionomycin was utilized to produce a robust Ca^{2+} signal.

4.1.1. TRPM5 current in rat ß-cells during ionomycin-induced Ca^{2+} mobilization

In our initial assessment of TRPM5 in pancreatic ß-cells from Wistar Kyoto and Goto Kakizaki rat, we utilized the Ca^{2+} ionophore, ionomycin, to stimulate Ca^{2+} release from the endoplasmic reticulum. Figure 1A displays the current collected at -80 millivolts

and at +80 millivolts. Upon Ca^{2+} mobilization from the endoplasmic reticulum, we observed an increase in both currents from both animals that reflected the TRPM5 signature, namely its transient activation and outward rectification. Currents from both animals displayed typical TRPM5 behavior of transient activitation. The current-voltage relationship exhibited in Figure 1B displayed the typical outward rectification of the TRPM5 current. The currents measured at +80 millivolts were considerably higher than the currents measured at -80 millivolts for both animal types. In addition, the current measured from the Goto Kakizaki rat at +80 millivolts was smaller than the current measured from the Wistar Kyoto rat at +80 millivolts. Several conclusions can be drawn from these data. While there are differences in current amplitude between the Wistar Kyoto and Goto Kakizaki rat pancreatic ß-cells, the transient nature of TRPM5 activation is retained in both ß-cell types. The differences exhibited between the current amplitudes of Wistar Kyoto and the Goto Kakizaki rat pancreatic ß-cells may be due to: (1) less expression of TRPM5 in Goto Kakizaki rats as opposed to the Wistar Kyoto rats, (2) dysfunctional TRPM5 channels in the Goto Kakizaki rat, (3) insufficent Ca^{2+} signaling in the Goto Kakizaki rat or a combination of all three.

4.1.2. Chronic Hyperglycemia Reduces Expression of Membrane Proteins

In a study performed by Jonas, et al. (1999), it was reported that ion channel and ion pump mRNA levels were markedly decreased in male Sprague-Dawley rats in which chronic hyperglycemia was induced. More specifically, the mRNA levels of the pore forming subunit of the ATP sensitive K^+ (K_{ATP}) channel (Kir6.2) was significantly reduced while the mRNA levels of the regulatory subunit (SUR1) was not significantly

affected. In addition, the mRNA level of the alpha subunit of the voltage-dependant Ca^{2+}-channel (VDCC) was also significantly decreased during chronic hyperglycemia. Kir6.2 and the alpha subunits listed above both form the pore regions of their respective ion channels. The pore forming subunits of channels are crucial in that they provide ion selectivity via ionic charge and/or size. If this portion of the ion channel has been reduced, then ion conductivity of the channel may not function properly, thereby rendering the channel unable to conduct ions. The results of our study may support the suggestion that the reduction in current amplitudes measured in Goto Kakizaki rat pancreatic ß-cells may be due to a reduced expression of TRPM5 due to chronic hyperglycemia.

4.1.3. Ca^{2+} Homeostasis, the SERCA Pump, TRPM5 and Chronic Hyperglycemia

Calcium plays a key role in normal pancreatic ß-cell function and its homeostasis within the ß-cell is crucial in maintaining cellular function. Under normal conditions, cytosolic free Ca^{2+} is approximately 100 nM while the free Ca^{2+} of the lumen of the endoplasmic reticulum ranges between 100-700 μM. Thus, there exists a very large free Ca^{2+} gradient between the lumen of the endoplasmic reticulum and the cytosol. It has been shown that the sarcoplasmic endoplasmic reticulum Ca^{2+}-ATPase (SERCA) pump plays a significant role in the clearance of calcium from the cytosol of mouse pancreatic ß-cell (Chen et al., 2003). The SERCA pump is significant in that it maintains a very large free calcium gradient across the ER lumen (from 100-700 μM) (Bygrave and Benedetti, 1996) and the cytosol (100 nM). This Ca^{2+} is held and released from the endoplasmic reticulum during certain cellular events and acts as a second messenger in

many cellular processes. SERCA replenishes the Ca^{2+} when the stores have been depleted. In addition, the activity of SERCA has been shown to play an important role in ß-cell Ca^{2+} signaling (Roe et al., 1994 and Worley et al., 1994).

TRPM5 is a channel activated by calcium. A cell at rest, has an intracellular Ca^{2+} concentration of about 100 nM. This intracellular Ca^{2+} concentration is insufficient for activating TRPM5. Therefore, there must be an increase in intracellular Ca^{2+} in order for TRPM5 activation to occur. Intracellular Ca^{2+} increase occurs via Ca^{2+} influx through various calcium ion channels like I_{crac} and VDCCs and through Ca^{2+} store depletion. In order to measure the cytosolic Ca^{2+}, we employed Fura-2 measurements in conjunction with whole-cell patch-clamp measurements. Fura-2 is a Ca^{2+}-sensitive ratiometric fluorophore. Figure 2A shows the Ca^{2+} signal generated from ionomycin application. Solubilizing ionomycin with 0-Ca^{2+}-Sodium Ringer allows us to make the assertion that the source of the Ca^{2+} signal is solely to Ca^{2+} release from the endoplasmic reticulum. The Ca^{2+} signal from Goto Kakizaki pancreatic ß-cell is significantly lower than the calcium signal generated in the Wistar Kyoto rat. In a previous study (Prawitt et al., 2003) involving the rat INS-1 cell line, it was shown that activation of the TRPM5 current is Ca^{2+} dependant. Therefore, we believe that TRPM5 is expressed in Wistar Kyoto rat pancreatic ß-cells and we also believe the reduced activation of TRPM5 in the Goto Kakizaki rat pancreatic ß-cells may be associated with the reduction of the Ca^{2+} signal in these cells. The lower Ca^{2+} signal generated in the Goto Kakizaki rat may be due to the effects of chronic hyperglycemia. In addition to the negative effect of chronic hyperglycemia on mRNA levels of ion channels, Jonas, et al. (1999) reported that chronic hyperglycemia also adversely affected mRNA levels of the third isoform of the

sarcoendoplasmic reticulum Ca^{2+}-ATPase (SERCA) pump in male Sprague-Dawley rats. Data from a study conducted by Kono, et al. (2012), reports a loss of expression of SERCA pump isoform 2b in several diabetes models from mice and cadaveric human islets. They concluded that the decrease in SERCA2 isoform expression is directly correlated with diabetes severity.

The Goto Kakizaki rat is a non-obese type 2 diabetic mouse model. One of the characteristics of the Goto Kakizaki rat is that it has chronic hyperglycemia (Beddow and Samuel, 2012). Therefore, the reduction in the ionomycin-induced Ca^{2+} signal exhibited in the Goto Kakizaki rat pancreatic ß-cell reflects a reduction in the amount of Ca^{2+} stored in the endoplasmic reticulum that may be explained by a downregulation of SERCA pump expression (thus a dysfunctional store refilling and reduced calcium signal) leading to adverse effects on pancreatic ß-cell function.

4.2. TRPM5 EXPRESSION

The expression of TRPM5 is widespread and occurs across a variety of tissues. TRPM5 was initally reported to be expressed in a subset of mammalian tastebuds playing a role in the transduction of bitter, sweet and umani tastes (Perez et al. 2002; Zhang et al. 2003). In subsequent studies, TRPM5 expression was detected and described in olfactory neurons (Lin et al., 2007; Hansen and Finger 2008) for the detection of semiochemicals and pheromones, in the gastrointestinal tract (Kaske et al., 2007) and the respiratory system (Kaske et al., 2007) for recognizing and processing envrionmental cues, in Purkinje cells (Kim et al. 2012) for contributing to the depolarization-induced slow current and in pancreatic ß-cells (Brixel et al. 2010) for playing a role in insulin secretion.

4.2.1. K14D10 identifies viable rat pancreatic ß-cells and TRPM5 antibody is specific

We incorporated immunostaining to determine the viability of the pancreatic ß-cells following isolation. K14D10, is a highly specific rat pancreatic ß-cell surface antibody (Hadjvassiliou et al., 2000). Figures 3A and 3B show (in red) very distinct staining with K14D10 on the surface of a population of the isolated rat pancreatic ß-cells from both Wistar Kyoto and Goto Kakizaki rats, respectively. Not only does K14D10 identify pancreatic ß-cells but it also determines cell viability. With this in mind, we were able to conclude that our isolation procedures resulted in a highly purified and viable population of pancreatic ß-cells from Wistar Kyoto and Goto Kakizaki rats.

The results obtained from the Wistar Kyoto rat spleen cells (Figure 5) provided information regarding the specificity of the K14D10 and TRPM5 antibodies. We utilized the spleen cells as a negative control for K14D10 and to rule out non-specific binding of the TRPM5 antibody to TRPM4. TRPM4 is closely related to and shares 40% structural homology with TRPM5. TRPM4 has been shown to be moderately expressed in the spleen of the rat (Yoo et al., 2010). If the TRPM5 antibody was non-specific, thereby binding to TRPM4 that was shown to be expressed in the rat spleen, then the spleen cells from the Wistar Kyoto rat would show some fluorescence. As displayed in Figure 5, there was no detectable fluorescence due to binding of K14D10 and TRPM5 antibodies. Therefore, the K14D10 antibody and the TRPM5 antibody are specific for the identification of viable pancreatic ß-cells and TRPM5, respectively.

4.2.2. TRPM5 is not localized to the membrane of non-stimulated pancreatic ß-cells

Figure 3A displays the staining results of an antibody specific to TRPM5 (green) in Wistar Kyoto pancreatic ß-cells. This data shows TRPM5 to be homogeneously expressed and dispersed throughout the cytosol of the rat pancreatic ß-cells. TRPM5 shares 40% homology with its close relative, TRPM4. TRPM4 is a calcium-activated, monovalent cation channel. Moreover, TRPM4 has been shown to be expressed in the INS-1 cell line, a rat pancreatic ß-cell line and to be involved in insulin secretion (Cheng et al., 2007). In this study, TRPM4 was observed to have two phases of activation. During the second phase of activation, the increase in the TRPM4 current was accompanied with an increase in cell capacitance. Cell capacitance measures the size of the cell and an increase in cell capacitance is indicative of exocytosis. Therefore, this study showed that TRPM4 was translocated to the cell membrane during the second phase of current activation. It is plausible that the TRPM5 proteins behave similar to TRPM4 in that they are located in the cytosol and upon receiving stimulus, may be translocated to the membrane. This hypothesis is supported by the fact that in our patch-clamp experiments, which allows us to measure ion flux across the plasma membrane, we were able to detect functional TRPM5 channels upon calcium stimulation.

Although our follow-up staining experiments examining whether stimulating pancreatic ß-cells may result in the translocation of TRPM5 to the membrane were inconclusive, Figure 11 shows the change in capacitance (pink trace) of ß-cells during intracellular perfusion with 6 μM Ca^{2+}. This increase in capacitance was associated with the activation of the TRPM5 current (black trace) which would suggest that activation of TRPM5 occurs simultaneous to the translocation of TRPM5 to the membrane via

exocytosis. Both of these processes are Ca^{2+} dependant. The Goto Kakizaki rat pancreatic ß-cells exhibited a very slight increase in both current and capacitance (Figure 11B). This significant reduction in current and capacitance may be due to the absence or reduction of TRPM5 channels and/or other proteins involved in exocytosis such as SNARE proteins, respectively.

An interesting observation of Figure 11A is that although the capacitance increases and is sustained at a constant value suggesting the presence of TRPM5 in the plasma membrane and although Ca^{2+} is still present, the TRPM5 current is transient. The transient nature of the current is important in insulin secretion. Insulin secretion from pancreatic ß-cells is pulsatile and is caused by intracellular Ca^{2+} oscillations. These intracellular Ca^{2+} oscillations are controlled by the voltage-dependant Ca^{2+} channels which depends on the cell's membrane potential. Colsoul et al. (2010) have shown that the islet cells from TRPM5 knockout mice ($TRPM5^{-/-}$) displayed a loss in the fast oscillations required to contribute to membrane depolarization. Therefore, the transient nature of the rat TRPM5 may play a role in depolarizing the membrane of the ß-cells to elicit the Ca^{2+} oscillations required for insulin secretion.

4.2.3. TRPM5 is not expressed in GK rat ß-cells and under hyperglycemic conditions

Figure 3B displays the results of the same staining procedure as performed in figure 3A. The Goto Kakizaki rat pancreatic cells were identified with the K14D10 antibody. In our studies of TRPM5 expression in pancreatic ß-cells from the Goto Kakizaki rat, we found TRPM5 expression to be reduced to undetectable levels. Because the staining experiments shown in figure 3 were done in parallel, we can ascertain that

the images obtained are due to the actual expression of the cell and not due to variations in treatment. This reduction to undectable levels may be due to the fact that the Goto Kakizaki rat is characterized as having chronic hyperglycemia and it has been previously mentioned that this condition leads to a reduction in the expression of TRPM5.

In addition to the data showing the diabetic pancreatic ß-cell having undectable levels of TRPM5, we have shown the effect (Figure 4) of a 16-hour incubation in 10 mM glucose on TRPM5 expression in Wistar Kyoto rat pancreatic ß-cells. Therefore, we conclude chronic hyperglycemic conditions cause a reduction in the expression of TRPM5.

4.3. GLUCOSE STIMULATION AND THE CA^{2+} RESPONSE

The pancreatic ß-cell is an electrically excitable cell which transduces changes in blood glucose into changes in cytosolic free Ca^{2+} which ultimately leads to the secretion of insulin. In the islet of Langerhans, glucose stimulation leads to Ca^{2+} oscillations that are a result of membrane potential oscillations that induce intermittent Ca^{2+} influx through voltage-dependant Ca^{2+} channels (Gilon and Henquin, 1992). Therefore, insulin secretion in pancreatic ß-cell involves the complex interplay between ion channels and transporters (MacDonald and Rorsman, 2006). As blood glucose rises, glucose enters the pancreatic ß-cell via the GLUT-2 plasma membrane transporter (Berne and Levy, 1998). The metabolism of glucose results in the production of ATP, thereby closing ATP-sensitive K^+ channels (K_{ATP}) and initiating the depolarization of the plasma membrane (Rorsman and Trube, 1985). This voltage change leads to the activation of voltage-operated Ca^{2+} channels. During the activation of the voltage-operated Ca^{2+} channels,

Ca^{2+}-induced Ca^{2+} release from the endoplasmic reticulum amplifies the Ca^{2+} signal (Lemmens, et al., 2001), which ultimately results in insulin secretion. The studies conducted in Figure 6 were performed to compare the Ca^{2+} signals generated with a stimulatory concentration of glucose between pancreatic ß-cells of Wistar Kyoto and Goto Kakizaki rats cultured under normal- and hyper- glycemic conditions.

4.3.1. The Ca^{2+} signal of Wistar Kyoto pancreatic ß-cells stimulated with glucose

Under normal glucose growth conditions, the results of figure 6A show a moderate increase in intracellular Ca^{2+} during extracellular exposure of the Wistar Kyoto pancreatic ß-cell to a stimulatory concentration of glucose. While other groups (Gilon and Henquin, 1992) have reported oscillations in intracallular Ca^{2+} during exposure of pancreatic ß-cells to stimulatory concentrations of glucose, it is important to note that their experiments were performed in intact islets or clusters of ß-cells. Our studies were performed on isolated single ß-cells. Beta cells make up approximately 90% of the islet and are interconnected via gap junctions which mediate the coupling and synchronization of intracellular Ca^{2+} oscillations (Grapengiesser et al., 2004). In individual mouse pancreatic ß-cells, Hellman (2009) reports that ß-cells lacking contact with other cells exhibit oscillatory frequency which differs considerably from ß-cells that were situated in aggregates. In addition, it was reported (Grapengiesser et al., 1989) that the glucose sensitivity of individual ß-cells varies and that the patterns of rhythmic depolarizations are a result of the electrically coupled cells within the islet. Moreover, a study conducted by Zhao et al., (2003), demonstrates a marked difference between the Ca^{2+} signals generated from mice and rats when stimulated with glucose. The mouse glucose-induced

Ca^{2+} signal was fast, robust and moderately oscillatory. The rat Ca^{2+} signal, on the other hand, was slow, smaller and short-lived. Our data are consistent with the findings mentioned above in that the oscillatory nature of a single rat ß-cell was completely lost and the Ca^{2+} increase was slow and gradual.

When cultured under hyper-glucose (10 mM) conditions for at least 16 hours, the Wistar Kyoto pancreatic ß-cell Ca^{2+} response (Figure 6B) to glucose is dysfunctional. The Ca^{2+} response from Wistar Kyoto ß-cell to glucose was identical to the control cells that were exposed to extracellular saline. The fact that the control cells (saline) exhibited almost identical signals as the cells that were stimulated with glucose indicates that preincubation with hyper-glucose growth conditions resulted in the disruption of Ca^{2+} homeostasis. This aberration in cytosolic Ca^{2+} may be due to increased basal metabolism and hypersensitivity to glucose (Olofsson et al., 2007; Khaldi et al., 2004). The hyper-glucose-induced disruption of Ca^{2+} homeostatsis may also be the secondary effect of other pathways and mechanisms including: increased oxidative stress, increased glucosamine pathway activity, increased ER stress, accelerated glucolipotoxicity, glycation stress, activation of inflammatory pathways and toxic accumulation of islet amyloid polypeptide (Prentki and Nolan, 2006).

4.3.2. The Ca^{2+} signal of Goto Kakizaki pancreatic ß-cells stimulated with glucose

Figure 7B depicts the glucose-stimulated Ca^{2+} signal in Goto Kakizaki rat pancreatic ß-cells that were subjected to an overnight incubation in growth media that contained 10 mM glucose. The 10 mM growth conditions are similar to what Goto Kakizaki rat ß-cells are exposed to in vivo. When exposed to a stimulatory concentration

of glucose (16.7 mM), the resulting Ca^{2+} signal was robust, surpassing the glucose-stimulated Ca^{2+} signal measured in the Wistar Kyoto rat ß-cells (Figure 6A). These data conflict with other studies (Yasuda et al., 2002) which demonstrate the control cells exhibiting a much larger response than that of the Goto Kakizaki rat. The Yasuda study showed that while the Goto Kakizaki rat ß-cells did in-fact respond to stimulatory glucose, the Wistar Kyoto rat ß-cells showed a much larger response. Therefore, it may be possible that the Wistar Kyoto response exhibited in Figure 6A may be uncharacteristic of most studies carried out in similar fashion. One must also keep in mind that the changes in intracellular Ca^{2+} due to glucose stimulation elicit heterogeneous responses (Yasuda et al., 2002). Thus, it is possible that the records in Figure 6A reflect a subpopulation of potential responses in the Wistar Kyoto ß-cell.

The experiments performed in figure 7A show the response of the Goto Kakizaki rat pancreatic ß-cells to stimulation with glucose following an overnight incubation in 4 mM glucose. The overnight incubation in 4 mM could be construed as an attempt to rescue cells from a chronic hyperglycemic environment. Matsuda et al., (2002) showed that Wistar Kyoto rat ß-cells which were streptozotocin-induced into a diabetic state and then subsequently treated for 6 weeks with diazoxide showed a marked protection against progression of diabetes. The results of figure 7A demonstrate a distinct difference between ß-cells of the Goto Kakizaki subjected to overnight glucose concentration of 10 mM and 4 mM. The Ca^{2+} response of the Goto Kakizaki pancreatic ß-cells subjected to an overnight incubation of 4 mM glucose resembled the response

observed in the Wistar Kyoto pancreatic ß-cells, which suggests that intervention with a normal glucose concentration, even after the development of diabetes, may improve the state of the diabetic cell.

4.4. CARBACHOL, CA^{2+} RELEASE AND TRPM5

As previously mentioned in the Introduction, the parasympathetic nervous system is involved in insulin secretion through the release of acetylcholine. In addition, pancreatic ß-cells express the m3, muscarinic receptor. Involvement of the parasympathetic system has been shown to occur immediately following a meal in rats and humans, even before the rise of blood glucose, suggesting a role in the potentiation of glucose-stimulated insulin secretion (Ahren et al., 1990; Stubbe et al., 1993) and in providing a signal in keeping the ß-cell responsive to the anticipated glucose challenges (Rodriguez-Diaz et al., 2012). Upon stimulation with acetylcholine, the m3 muscarinic receptor, initiates the production of IP3 production and IP3 binds to the IP3 receptor of the endoplasmic reticulum to trigger Ca^{2+} release. Carbachol is an agent that mimics acetylcholine. Carbachol was utilized due to the inability of cholinesterase to metabolize it.

4.4.1. The Ca^{2+} signal of WK and GK pancreatic ß-cells stimulated with carbachol

Figure 8A depicts the calcium signal generated from Wistar Kyoto and Goto Kakizaki rat pancreatic ß-cells given extracellular stimulation of carbachol. As shown in the figure, the Ca^{2+} signals from both populations of cells are nearly identical. Although baseline Ca^{2+} differed amoung the two populations of cells, following stimulation, both

populations of cells reached a maximum Ca^{2+} signal of approximately 450 nM Ca^{2+}. Following the initial rise, the secondary Ca^{2+} signal of the Goto Kakizaki rat deviated from the secondary Ca^{2+} signal of the Wistar Kyoto. Typically, this secondary response involves the activation of store-operated channels, located within the plasma membrane. The initial Ca^{2+} response to carbachol stimulation being nearly identical between both populations showed that the M3 muscarinic receptor expression and function in Goto Kakizaki rats remained intact and was not affected by chronic hyperglycemia. In addition, the IP3 receptors in the endoplasmic reticulum of the Goto Kakizaki rat were also not affected by chronic hyperglycemia. The deviation of the secondary Ca^{2+} signal in the Goto Kakizaki rat may be an indication that the Ca^{2+} Release-Activated Ca^{2+} Current (I_{CRAC}) may be affected by chronic hyperglycemia.

The amplitude of the carbachol-induced calcium signal is noticeably smaller than the ionomycin-induced calcium signal. It has been estimated (Bygrave and Benedetti, 1996) that the agonist-releasable Ca^{2+} concentration in the ER is approximately 0.5-1.0 mM. Figure 2A shows the Ca^{2+} signal reaching a minimum of 2 μM, which does not come close to the estimated concentration. Ionomycin targets cell membranes. Although its target is specific, the actual number of ionomycin molecules that are inserted into the membrane is non-specific and unknown. On the other hand, the M3 muscarinic receptor is located within the plasma membrane and there is a finite level of expression which when stimulated with a saturating amount of carbachol, results in the production of IP3. The IP3 receptors in the endoplasmic reticulum also exhibit finite expression and may elicit a Ca^{2+} signal that may not reflect the actual Ca^{2+} concentration within the stores.

The differences in measured release from the Ca^{2+} stores elicited via ionomycin and carbachol may be explained by the differences in ionophore insertion into the membrane compared to the expression of receptors.

4.4.2. The Ca^{2+} signal of WK and GK pancreatic ß-cells and TRPM5 activation

TRPM5 is a Ca^{2+} activated channel. In spite of having a lower agonist-induced Ca^{2+} signal in both populations of cells, that signal was sufficient to activate a small TRPM-like current. In a previous study (Prawitt et al., 2003), TRPM5 was shown to respond to rapid changes in Ca^{2+} concentrations. In Wistar Kyoto and Goto Kakizaki rat pancreatic ß-cells, the carbachol-induced Ca^{2+} response exhibits a rapid change in intracellular Ca^{2+} concentration. In this case of TRPM5 activation in Wistar Kyoto and Goto Kakizaki rat pancreatic ß-cells, the Ca^{2+} signal was sufficient to activate TRPM5 and this may have been due its rapid intracellular increase. It is also important to note that the Fura-2 Ca^{2+} signal is the average Ca^{2+} concentration measured across the cell and that localized changes in Ca^{2+} may be higher. Although there is no significant difference in the carbachol-induced Ca^{2+} signal, the difference in the elicited TRPM5 may be explained only by the difference in expression between the Goto Kakizaki and Wistar Kyoto pancreatic ß-cells.

The carbachol-induced TRPM5 current from the Wistar Kyoto pancreatic ß-cells show the typical transient nature of the current reported previously. TRPM5 is a non-specific monovalent cation channel that conducts sodium ions into the cell. The pancreatic ß-cell is an electrically excitable cell, able to produce action potentials. These action potentials are important in the recruitment of voltage-gated Ca^{2+} channels that

have been shown to induce insulin secretion. The movement of sodium ions into the cell via TRPM5 would shift the membrane to a more positive potential, thereby contributing to depolarization of the membrane. Insulin secretion has been shown to occur in a pulsatile manner, occuring in-sync with intracellular Ca^{2+} oscillations which mirror the electrical oscillations of the membrane. TRPM5 may contribute to membrane depolarization and due to its transient nature may contribute to the electrical oscillations observed during insulin secretion.

4.4.3. Acetylcholine, the Ca^{2+} signal, TRPM5 activation and the membrane potential

Acetylcholine plays an important role in insulin secretion in the preabsorptive and absorptive phase of food intake (Ahren, 2000; Gilon and Henquin, 2001). During the preabsorptive phase of food digestion, before blood glucose has increased, the vagus nerve is activated in response to input from sensory organs located in the oral cavity and the visual and olfactory systems. This initial stimulation of the M3 muscarinic receptor produces IP3 and protein kinase C (PKC). IP3 mobilizes Ca^{2+} and PKC mediates the efficiency of Ca^{2+} during exocytosis of the readily releasable pools of insulin-containing vesicles that have been shown to be in close proximity to the membrane. During the absorptive phase of food intake, when blood glucose has increased and the pancreatic ß-cell has been exposed to glucose, acetylcholine still acts on the M3 muscarinic receptor. In this case, however, the mobilization of Ca^{2+} results in the activation of TRPM5. At the same time, glucose has been metabolized to produce ATP, leading to the closure of ATP-sensitive K^+ (K_{ATP}) channels. Being that TRPM5 conducts an inward sodium current, its

activation works synergistically with the closure of the K_{ATP} channel, which together, provide sufficient depolarization of the pancreatic ß-cell to initiate glucose-stimulated insulin secretion.

4.4.4. Passive store depletion does not activate TRPM5 in rat pancreatic ß-cells

There are conflicting reports regarding TRPM5's activation mechanism (Perez et al., 2002; Prawitt et al., 2003). The contradiction is whether TRPM5 is store-operated or Ca^{2+}-activated. Figure 12 shows the effect of perfusion of a Ca^{2+} chelator (DiBromo-BAPTA) on TRPM5 activation in the Wistar Kyoto pancreatic ß-cell. Because there is no significant development of any current, the statement can be made that TRPM5 in pancreatic ß-cells if the Wistar Kyoto rat is not activated by passive store depletion. This observation is in agreement with a previous study performed by our group (Prawitt et al., 2003) on the insulinoma rat cell line.

4.5. CA^{2+} DOSE RESPONSE OF TRPM5 IN WK AND GK RATS

4.5.1. The Ca^{2+} dose response of TRPM5

The Ca^{2+} dose response of the TRPM5 channel in pancreatic ß-cells of Wistar Kyoto and Goto Kakizaki rats both display a sigmoidal shape which is characteristic of cooperative binding of Ca^{2+} molecules to the TRPM5 protein. A reduction in the I_{max} of TRPM5 in the Goto Kakizaki rat pancreatic ß-cells may be an indication that either there are less channels available to carry the current or that the channels are dysfunctional. The decrease in I_{max} displayed by the Goto Kakizaki rat pancreatic ß-cells again reinforces the earlier finding of a reduction in TRPM5 in these cells. Although there is a reduction

in the I_{max}, the affinity of calcium to TRPM5 and the Hill coefficient in Goto Kakizaki pancreatic ß-cells are both increased. These observations, taken together, support the idea that chronic hyperglycemia affects expression and function of the TRPM5 channel.

4.5.2. The differences in the carbachol-induced and Ca^{2+} dose response of TRPM5

While the K_m for Ca^{2+} to activate TRPM5 is 4.89 μM, the concentration of calcium measured during agonist stimulation with carbachol peaked at 457 nM. When the agonist-induced Ca^{2+} signal is utilized to extrapolate a current size from the Ca^{2+} dose response curve, the values are disproportional. As mentioned earlier, this can be explained because the Fura-2 Ca^{2+} signal generated from carbachol stimulation represents the average signal across the entire cell. Localized Ca^{2+} changes may be higher.

4.5.3. The Ca^{2+} dose response of TRPM5 and the increase in capacitance

Aside from gathering information regarding the activation kinetics of TRPM5 in Wistar Kyoto and Goto Kakizaki pancreatic ß-cells, we were also able to observe the increase in capacitance during intracelluar perfusion with various concentrations of free Ca^{2+}. The increase in capacitance is an indication of an increase in the surface area of the cell membrane which is an indication of exocytosis. The secretion of insulin from pancreatic ß-cells requires exocytosis. We have hypothesized that TRPM5-containing vesicles may also undergo membrane fusion upon Ca^{2+} stimulation. Cheng et al., (2007) have shown that perfusion of INS-1 rat pancreatic ß-cells with Ca^{2+} initiates both insulin secretion and translocation of TRPM4-containing vesicles to the plasma membrane. Furthermore, the increase in capacitance due to TRPM4-containing vesicles was

accompanied with increases in current. Our data show the activation of a transient TRPM5 current occuring simultaneous with an increase in capacitance. Thus, we believe the capacitance change observed is associated with the recruitment of TRPM5-containing vesicles to the membrane. Because we did not observe any change in capacitance during carbachol stimulation or during perfusion with 1 μM free Ca^{2+} (data not shown), we believe the recruitment of TRPM5-containing vesicles occurs at free Ca^{2+} concentrations greater than 3 μM.

CHAPTER 5. CONCLUSIONS & PROSPECTIVE STUDIES

5.1. TRPM5 IN WK AND GK RAT ß-CELLS

Our work has shown Wistar Kyoto rat pancreatic ß-cells express the ion channel TRPM5. The TRPM5 channel expressed in the Wistar Kyoto rat pancreatic ß-cell exhibits the features previously studied by our group in the HEK-293 overexpressed system as well as in the rat insulinoma cell line (INS-1), namely Ca^{2+}-activated and transient activation (Prawitt et al., 2003). We have also shown that the Goto Kakizaki rat pancreatic ß-cells exhibit a reduction in the expression of TRPM5 which may be a result of chronic hyperglycemia. The reduction in expression leads to pancreatic ß-cell dysfunction which may exacerbate the progression of the disease.

5.1.1. TRPM5 is a Ca^{2+}-activated transient current and not store-operated

We were able to measure intracellular Ca^{2+} concentrations in conjunction with measuring ion fluxes across the plasma membrane and into pancreatic ß-cells. We showed that TRPM5 is a transient current activated by an increase in intracellular Ca^{2+}. We also demonstrated that this activation was dose dependant, where we measured larger TRPM5 currents with larger intracellular Ca^{2+} concentrations.

TRPM5 was also activated by release of Ca^{2+} from the endoplasmic reticulum. We believe that this activation was due to Ca^{2+} ions and not due to store depletion. We demonstrate this with perfusion of the Wistar Kyoto rat pancreatic ß-cell with a Cesium-based ringer containing 10 mM Di-Bromo BAPTA which resulted in no measurable current that resembled TRPM5.

5.1.2. The transient nature of TRPM5 provides a mechanism for initiating oscillations

It is widely accepted that oscillations in intracellular Ca^{2+} and membrane potential in the pancreatic ß-cell are necessary in insulin secretion. In order for these oscillatory events to be orchestrated and maintained, glucose, neurotransmitters, ion channels, transporters and a vast array of intracellular and membrane proteins play various roles in the secretion of insulin to maintain blood glucose homeostasis. We have been able to make a physiological connection between TRPM5 and its possible role in insulin secretion in the Wistar Kyoto rat pancreatic ß-cells as contributing to the depolarization of the plasma membrane in the later recruitment of the voltage-operated Ca^{2+} channels which lead to insulin secretion. Due to its transient nature, we also believe TRPM5 to play a role in the electrical oscillations that are very apparent during insulin secretion.

Schematic diagram 2 illustrates the role of TRPM5 in insulin secretion. The diagram illustrates that parasympathetic stimulation of the M3 muscarinic receptor occurs prior to the rise in blood glucose to stimulate Ca^{2+} release from the endoplasmic reticulum and subsequent activation of TRPM5. This activation brings the potential of the ß-cell plasma membrane to a more positive potential. When glucose uptake occurs, ATP levels within the cell lead to the closure of the K_{ATP} channel. Closing of the K_{ATP} channel together with the activation of TRPM5 pushes the membrane potential past its threshold to initiate membrane depolarization. This depolarization results in the recruitment of voltage-activated Ca^{2+} channels and the influx of Ca^{2+} to stimulate insulin secretion.

5.1.3. The Goto Kakizaki rat and TRPM5 expression

In the type 2 diabetes, cells are chronically exposed to hyperglycemia. This chronic exposure to high glucose has many devastating effects on cellular proteins of the pancreatic ß-cells. In the hyperglycemic state, the glycolytic capacity of the mitochondria is exceeded and anaerobic glycolysis results in the excessive production of reactive oxygen species (ROS), which leads to chronic oxidative stress (Robertson et al., 2003). Elevated ROS have been shown to disturb the integrity and function of cellular proteins and DNA. Therefore, the reduced expression observed in Goto Kakizaki rat pancreatic ß-cells may be due to the effects of elevated ROS.

5.2. PROSPECTIVE STUDIES

5.2.1. TRPM5 expression, membrane translocation, depolarization and insulin secretion.

- Because we show a decrease in TRPM5 expression in Wistar Kyoto pancreatic ß-cells following an overnight incubation in high glucose growth media, it would be interesting to see whether re-introducing pancreatic ß-cells to normal glucose levels could result in the rescue of the TRPM5 channel.
- We have shown an increase in capacitance when cells were perfused with high concentrations of free Ca^{2+}. We would like to examine whether stimulating the cells with ionomycin prior to fixing and staining may result in the translocation of TRPM5 to the plasma membrane thereby being able to detect more TRPM5 expression in the plasma membrane.

- Being that TRPM5 contributes to membrane depolarization, we can visualize this depolarization with the use of membrane potential sensitive dyes and the FDSS. Compare the degree of depolarization from both populations of cells.
- Compare the insulin secretion in Wistar Kyoto and Goto Kakizaki pancreatic ß-cells by measuring insulin content in the supernatant following TRPM5 activation.
- Determine the mechanism by which chronic hyperglycemia induces the downregulation of TRPM5 expression.

5.2.2. Comparative study of TRPM5 in WK and GK ß-cells prior to 14 weeks of age

- Because Goto Kakizaki rats do not develop type 2 diabetes until at least 14 weeks of age, it would be interesting to compare TRPM5 expression and function in the Wistar Kyoto and the Goto Kakizaki rat pancreatic ß-cells prior to age 14 weeks.
- Overexpress TRPM5 in Goto Kakizaki rat that have developed type 2 diabetes and observe if this counteracts the disease.

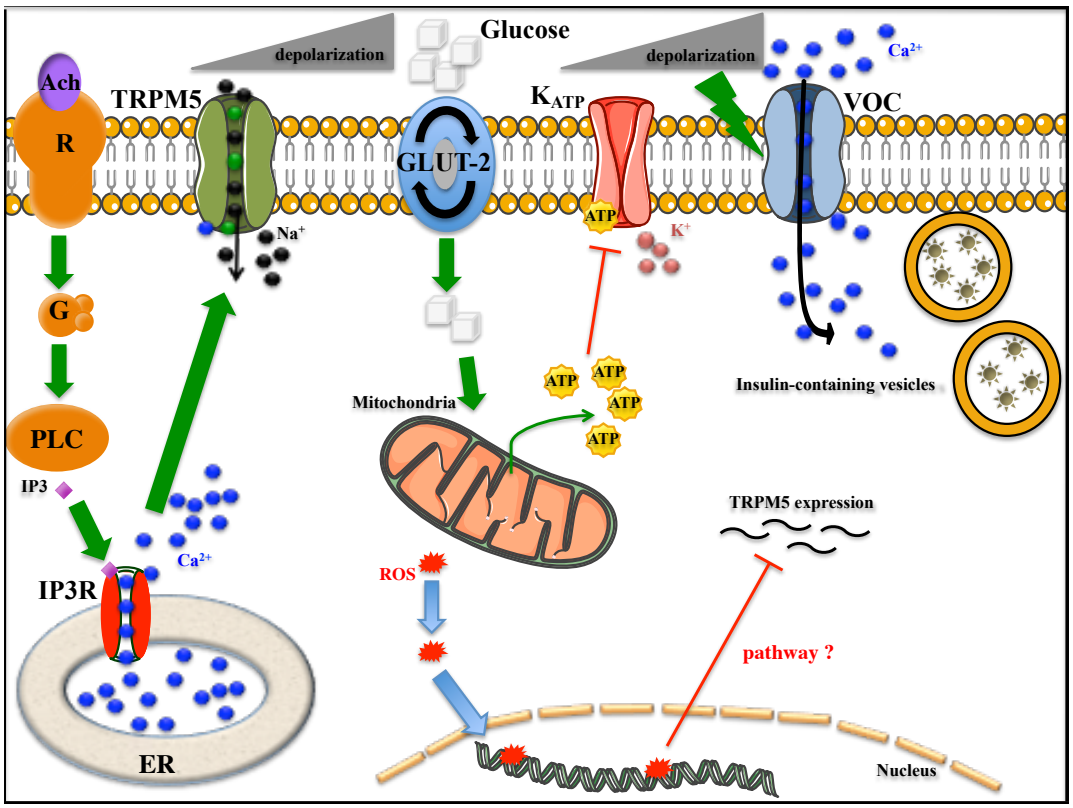

Diagram 2. Role of TRPM5 and hyperglycemia in insulin secretion. TRPM5 is activated by Ca^{2+} mobilization from the ER during preprandial M3 receptor stimulation from the parasympathetic nervous system. The activation of TRPM5 brings the membrane potential closer to the threshhold required to produce an action potential. Glucose metabolism increases intracellular ATP, the K_{ATP} channel closes and brings the membrane potential to threshold and the membrane depolarizes. This depolarization recruits voltage operated Ca^{2+} channels and that Ca^{2+} is involved in insulin secretion. When cells become chronically exposed to high glucose levels an increase of metabolic flux into the mitochondria induces excessive generation of reactive oxygen species (ROS), which leads to chronic oxidative stress. Elevated ROS have been shown to disturb the integrity and function of cellular proteins and DNA.

REFERENCES

Abdul-Ghani MA, Tripathy D, DeFronzo RA. (2006) Contributions of ß-cell dysfunction and insulin resistance to the pathogenesis of impaired glucose tolerance and impaired fasting glucose. Diabetes Care *29* (5), 1130-1139.

Ahren B. (2000) Autonomic regulation of islet hormone secretion-implications for health and disease. Diabetologia *43*, 393-410.

Ahren B, Karlsson S, Lindskog S. (1990) Cholinergic regulation of the endocrine pancreas. Prog Brain Res *84*, 209-218.

Ashcroft FM. (2000) Ion Channels and Disease. Academic Press, California. 25-31.

Ashcroft FM, Kelly R, Smith P. (1990b) Two types of Ca channel in rat pancreatic ß-cells. Pflugers Arch. *415*, 504-506.

Ashcroft FM, Rorsman P. (1989) Electrophysiology of the pancreatic ß-cell. Prog Biophys Mol Biol, *54*, 87-143.

Baetens D, Malaisse-Lagae F, Perrelet A, Orci L. (1979) Endocrine pancreas: three-dimensional reconstruction shows two types of islets of Langerhans. Science *206*, 1323-1325.

Beddow SA, Samuel VT. (2012) Fasting hyperglycemia in the Goto-Kakizaki rat is dependent on corticosterone:a confounding variable in rodent models of type 2 diabetes. Disease Models and Mechanisms *5* (5), 681-685.

Bell GI, Polonsky KS. (2001) Diabetes melitus and genetically programmed defects in ß-cell function. Nature *414*, 788-791.

Bisbis S, Bailbe D, Tormo MA, Picarel-Blanchot F, Derouet M, Simon J, Portha B. (1993) Insulin resistance in the GK rat: decreased receptor number but normal kinase activity in liver. Am J Physiol *265*, E807-E813.

Bonner-Weir S. (1989) Pancreatic islets: morphology, organization and physiological implications. Molecular and Cellular Biology of Diabetes Mellitus. Alan R. Liss, Inc., New York. 1-11.

Boschero AC, Szpak-Glasman M, Carneiro EM, Bordin S, Paul I, Rojas E, Atwater I. (1995) Oxotremorine-m potentiation of glucose-induced insulin release from rat islets involves M3 muscarinic receptors. Am J Physiol *268*, E336-E342.

Brunicardi FC, Sun YS, Druck P, Goulet RJ, Elahi D, Andersen DK. (1987) Splanchnic neural regulation of insulin and glucagon secretion in the isolated perfused human pancreas. Am J Surg *153*, 34-40.

Bygrave FL, Benedetti A. (1996) What is the concentration of calcium ions in the endoplasmic reticulum. Cell Calcium *19* (6), 547-551.

Cernea S and Dobreanu M. (2013) Diabetes and beta cell function: from mechanisms to evaluation and clinical implications. Biochemia Medica *23* (3), 266-280.

Chen L, Koh DS, Hille B. (2003) Dynamics of Calcium Clearance in Mouse Pancreatic β-cells. Diabetes *52*, 1723-1731.

Cheng H, Beck A, Launay P, Gross SA, Stokes AJ, Kinet AJ, Fleig A, Penner R. (2007) TRPM4 controls insulin secretion in pancreatic beta-cells. Cell Calcium *41* (1), 51-61.

Colsoul B, Schraenen A, Lemaire K, Quintens R, Van Lommel L, Segal A, Owsianik G, Talavera K, Voets T, Margolskee RF, Kokrashvili Z, Gilon P, Nilius B, Schuit FC, Vennekens R. (2010) Loss of high-frequency glucose-induced Ca2+ oscillations in pancreatic islets correlates with impaired glucose tolerance in TRPM5 -/- mice. PNAS USA *107* (11) 5205-5213.

D'Ambra R, Surana M, Efrat S, Starr RG, Fleischer N. (1990) Regulation of insulin secretion from beta-cell lines derived from transgenic mice insulinomas resembles that of normal beta-cells. Endocrinology *126*, 2815-2822.

Dyachok O, Gylfe E. (2004) Ca^{2+}-induced Ca^{2+} release via inositol 1,4,5-triphosphate receptors is amplified by protein kinase A and triggers exocytosis in pancreatic beta-cells. J Biol Chem *279* (44), 45455-45461.

Freshney R. (1987) Culture of Animal Cells: A Manual of Basic Technique. Alan R. Liss, Inc., New York. 117.

Gilon P and Henquin JC (1992) Influence of membrane potential changes on cytoplasmic Ca^{2+} concentration in an electrically excitable cell, the insulin-secreting pancreatic β-cell. (1992) J Biol Chem *267*, 20713-20720.

Gilon P and Henquin JC (2001) Mechanisms and physiological significance of the cholinergic control of pancreatic beta-cell function. Endocr Rev *22* (5), 565-604.

Goto Y, Suzuki K, Sasaki M, Ono T, Abe S. (1988) GK rat as a model of non-obese, non-insulin-dependent diabetes: selective breeding over 35 generations. Frontiers in Diabetes Research: Lessons from Animal Diabetes II. Shafrir E Renold AE eds, John Libbey, London, 301-303.

Grapengiesser E, Dansk H, Hellman B. (2004) Pulses of external ATP aid to the synchronization of pancreatic β-cells by generating premature Ca^{2+} oscillations. Biochemical Pharmacology *68*, 667-674.

Grapengiesser E, Gylfe E, Hellman B. (1989) Glucose effects on cytoplasmic Ca^{2+} of individual pancreatic beta-cells recorded by two procedures for dual-wavelength fluorometry. Exp Clin Endocrinol *93* (2-3), 321-327.

Hadijvassiliou V, Green MH, Green IC. (2000) Immunomagnetic purification of beta cells from rat islets of Langerhans. Diabetologia *43* (9), 1170-1177.

Harteneck C, Plant T, Schultz G. (2000) From worm to man: three subfamilies of TRP channels. TINS *23*, 159-166.

Henquin JC, Meissner HP. (1984) Significance of ionic fluxes and changes in membrane potential for stimulus-secretion coupling in pancreatic ß-cells. Experientia *40*, 1043-1052.

Hille B. (2001) Ion Channels of Excitable Membranes. Sinauer Associates, Inc., Massachusetts. 2-21.

Hoffman T, Chubanov V, Gudermann T, Montell C. (2003) TRPM5 is a voltage-modulated and Ca^{2+}-activated monovalent selective cation channel. Curr Biol *13*, 1153-1158.

Huang CL. (2004) The transient receptor potential superfamily of ion channels. J Am Soc Nephrol *15*, 1690-1699.

Iismaa TP, Kerr EA, Wilson JR, Carpenter L, Sims N, Biden TJ. (2000) Quantitative and functional characterization of muscarinic receptor subtypes in insulin-secreting cell lines and rat pancreatic islets. Diabetes *49*, 392-398.

Kahn SE. (2003) The relative contributions of insulin resistance and beta-cell dysfunction to the pathophysiology of Type 2 diabetes. Diabetologia *46*, 3-19.
Ketterer C, Mussig K, Heni M, Dudziak K, Randrianarisoa E, Wagner R, Machicao F, Stefan N, Holst JJ, Fritsche A, Haring HU, Staiger H. (2011) Genetic variation within the TRPM5 locus associates with prediabetic phenotypes in subjects at increased risk for type 2 diabetes. Metabolism *60* (9), 1325-1333.

Khaldi MZ, Guiot Y, Gilon P, Henquin JC, Jonas JC. (2004) Increased glucose sensitivity of both triggering and amplifying pathways of insulin secretion in rat islets cultured for 1 wk in high glucose. Am J Physiol Endocrinol Metab *287* (2), E207-E217.

Kim YS, Kang E, Makino Y, Park S, Shin JH, Song H, Launay P, Linden DJ. (2013) Characterizing the conductance underlying depolarization-induced slow current in cerebellar Purkinje cells. J Neurophysiol *109* (4), 1174-1181.

Kono T, Ahn G, Moss DR, Gann L, Zarain-Herzberg A, Nishiki Y, Fueger PT, Ogihara T, Evans-Molina C. (2012) PPAR-Y activation restores pancreatic islet SERCA2 levels and prevents β-cell dysfunction under conditions of hyperglycemia and cytokine stress. Mol Endocrinol *26* (2), 257-271.

Krishnan K, Ma Z, Bjorklund A, Islam MS. (2014) Role of transient receptor potential melastatin-like subtype 5 channel in insulin secretion from rat β-cells. Pancreas *43* (4), 597-604.

Kruger DF, Martin CL, Sadler CE. (2006) New insights into glucose regulation. The Diabetes Educator *32*, 221-228.

Lemmens R, Larson O, Berggren PO, Islam MS. (2001) Ca^{2+} -induced Ca^{2+} release from the endoplasmic reticulum amplifies the Ca^{2+} signal mediated by activation of voltage-gated L-type Ca^{2+} channels in pancreatic beta cells. J Biol Chem *276* 9971-9977.

Liu D and Liman E. (2003) Ca^{2+} and phosphatidylinositol 4,5-bisphosphate regulate the taste transduction channel TRPM5. Proc Natl Acad Sci USA *100*, 15160-15165.

Liu TP, Yu PC, Liu IM, Tzeng TF, Cheng JT. (2002) Activation of muscarinic M1 receptors by acetylcholine to increase glucose uptake into cultured C2C12 cells. Auton Neurosci *96* (2), 113-118.

MacDonald PE, Rorsman P. (2006) Oscillations, intercellular coupling, and insulin secretion in pancreatic beta cells. PLoS Biol *4*, e49.

Matsuda M, Kawasaki F, Mikami Y, Takeuchi Y, Saito M, Eto M, Kaku K. (2002) Rescue of beta-cell exhaustion by diazoxide after the development of diabetes mellitus in rats with streptozotocin-induced diabetes. Eur J Pharmacol *453* (1), 141-148.

Meldolesi J, Pozzan T. (1998) The endoplasmic reticulum Ca^{2+} store: a view from the lumen. Trends Biochem Sci *23* (1), 10-14.

Miguel JC, Abdel-Wahab YH, Mathias PC, Flatt PR. (2002). Muscarinic receptor subtypes mediate stimulatory and paradoxical inhibitory effects on an insulin-secreting beta cell line. Biochim Biophys Acta *1569* (1-3), 45-50.

Minke B and Cook B. (2002) TRP channel proteins and signal transduction. Physiol Rev *82*, 429-472.

Montell C, Birnbaumer L, Flockerzi V, Bindels R, Bruford E, Caterina M, Clapham D, Harteneck C, Heller S, Julius D, Kojima I, Mori Y, Penner R, Prawitt D, Scharenberg, A., Schultz G, Shimizu N, and Zhu M. (2002). A unified nomenclature for the superfamily of TRP cation channels. Mol Cell *9*, 229-231.

Movassat J, Saulnier C, Serradas P, Portha B. (1997) Impaired development of pancreatic beta-cell mass is a primary event during the progression to diabetes in the GK rat. Diabetologia *40*, 916-925.

Olofsson CS, Collins S, Bengtsson M, Eliasson L, Salehi A, Shimomura K, Tarasov A, Holm C, Ashcroft F, Rorsman P. (2007) Long-term exposure to glucose and lipids inhibits glucose-induced insulin secretion downstream of granule fusion with plasma membrane. Diabetes *56* (7), 1888-1897.

Paek HK, Moise LJ, Morgan JR, Lysaght MJ. (2005) Origin of insulin secreted from islet-like cell clusters derived from murine embryonic stem cells. Cloning Stem Cells *7*, 226-231.

Perez C, Huang L, Rong M, Kozak J, Preuss A, Zhang H, Max M, and Margolskee R. (2002) A transient receptor potential channel expressed in taste receptor cells. Nat Neurosci *5*, 1169-1176.

Perraud AL, Fleig A, Dunn C, Bagley L, Launay P, Schmitz C, Stokes A, Zhu Q, Bessman M, Penner R, Kinet JP, Scharenberg A. (2001) ADP-ribose gating of the calcium-permeable LTRPC2 channel revealed by Nudix motif homology. Nature *411*, 596-600.

Portha B, Serradas P, Bailbe D, Suzuki K, Goto Y, Giroix MH. (1991) Beta-cell insensitivity to glucose in the GK rat, a spontaneous nonobese model for type II diabetes. Diabetes *40*, 486-491.

Prawitt D, Enklaar T, Klemm G, Gartner B, Spangenberg C, Winterpacht A, Higgins M, Pelletier J, and Zabel B. (2000) Identification and characterization of MTR1, a novel gene with homology to melastatin (MLSN1) and the trp gene family located in the BWS-WT2 critical region on chromosome 11p15.5 and showing allele-specific expression. Hum Mol Genet *9*, 203-216.

Prawitt D, Monteilh-Zoller M, Brixel L, Spangengerg C, Zable B, Fleig A, and Penner R. (2003) TRPM5 is a transient Ca2+-activated cation channel responding to rapid changes in $[Ca^{2+}]_i$. Proc Natl Acad Sci *100*, 15166-15171.

Robertson RP, Harmon J, Tran PO, Tanaka Y, Takahashi H. (2003) Glucose toxicity in beta cells: type 2 diabetes, good radicals gone bad, and the glutathione connection. Diabetes *52*, 581-587.

Rodriquez-Diaz R, Dando R, Jacques-Silva MC, Fachado A, Molina J, Abdulreda M, Ricordi C, Roper SD, Berggen PO and Caicedo A. (2012) Alpha cessl secrete acetylcholine as a non-neuronal paracrine signal prming human beta cell function. Nat Med *17* (7), 888-892.

Roe MW, Mertz RJ, Lancaster ME, Worley JF, Dukes ID. (1994) Thapsigargin inhibits the glucose-induced decrease of intracellular Ca2+ in mouse islets of Langerhans. Am J Physiol *266*, E852-E862.

Rojas E, Hidalgo J, Carroll RB, Atwater I. (1990) A new class of calcium channels activated by glucose in human pancreatic ß-cells. FEBS Letters *261*, 265-270.

Sala S, Matteson DR. (1990) Single-channel recordings of two types of calcium channels in rat pancreatic ß-cells. Biophysical Journal *58*, 567-571.

Smith PA, Rorsman P, Ashcroft FM. (1989b) Modulation of dihydropyridine-sensitive Ca^{2+}-channels by glucose metabolism in pancreatic ß-cells. Nature *342*, 550-553.

Stubbe JH, Steffens AB. (1993) Neural control of insulin secretion. Horm Metab Res *25*, 507-512.

Szollosi A, Nenquin M, Henquin JC. (2007) Overnight culture unmasks glucose-induced insulin secretion in mouse islets lacking ATP-sensitive K^+ channels by improving the triggering Ca^{2+} signal. J Biol Chem *282* (20), 14768-14776.

Tokuyama Y, Sturis J, DePaoli AM, Takeda J, Stoffel M, Tang J, Sun X, Polonsky KS, Bell GI. (1995) Evolution of beta-cell dysfunction in the male Zucker diabetic fatty rat. Diabetes *44*, 1447-1457.

Varadi A, Molnar E, Ostenson CG, Ashcroft SJH. (1996) Isoforms of endoplasmic reticulum Ca^{2+} - ATPase are differentially expressed in normal and diabetic islets of Langerhans. Biochem J *319*, 521-527.

Verspohl EJ, Tacke R, Mutschler E, Lambrecht G. (1990) Muscarinic receptor subtypes in rat pancreatic islets: binding and functional studies. Eur J Parmacol *178*, 303-311.

Voets T, Nilius B, Hoefs S, Van der Kemp AWCM, Droogmans G, Bindels R, Hoenderop J. (2003) TRPM6 forms the Mg^{2+} influx channel involved in intestinal and renal Mg^{2+} absorption. J Biol Chem *279* (1), 19-25.

Walder R, Landau D, Meyer P, Shalev H, Tsolia M, Borochowitz Z, Boetter M, Beck G, Englehardt R, Carmi R, and Sheffield V. (2002) Mutation of TRPM6 causes familial hypomagnesemia with secondary hypocalcemia. Nat Genet *31*, 171-174.

Weir GC and Bonner-Weir S. (1990) Islets of Langerhans: the puzzle on intraislet interactions and their relevance to diabetes. J Clin Invest *85*, 983-987.

Worley JFI, McIntyre MS, Spencer B, Mertz RJ, Roe MW, Dukes ID. (1994) Endoplasmic reticulum calcium store regulates membrane potential in mouse islet beta-cells. J Biol Chem *269*, 14359-14362.

Yasuda K, Okamoto Y, Nunoi K, Adachi T, Shihara N, Tamon A, Suzuki N, Mukai E, Fujimoto S, Oku A, Tsuda K, Seino Y. (2002) Normalization of cytoplasmic calcium response in pancreatic beta-cells of spontaneously diabetic GK rat by the treatment with T-1095, a specific inhibitor or renal Na+-glucose co-transporters. Horm Metab Res *34* (4), 217-221.

Yoo JC, Yarishkin OV, Hwang EM, Kim E, Kim DG, Park N, Hong SG, Park JY. (2010) Cloning and characterization of rat transient receptor potential-melastatin 4 (TRPM4). Biochemical and Biophysical Research Communications *391*, 806-811.

Zhang Y, Hoon M, Chandrashekar J, Mueller K, Cook B, Wu D, Zuker C, Ryba N. (2003) Coding of sweet, bitter, and umani tastes: different receptor cells sharing similar signaling pathways. Cell *112*, 293-301.

Zhao YF, Xu R, Hernandez M, Zhu Y, Chen C. (2003) Distinct intracellular Ca^{2+} response to extracellular adenosine triphosphate in pancreatic β-cells in rats and mice. Endocrine *22* (3), 185-192.

Zimmet P, Alberti KG, Shaw J. Global and societal implication of the diabetes epidemic. (2001) Nature *414*, 782-787.